

## CHAPTER 5 TABLE OF CONTENTS

Chapter 5 Table of Contents .....	i
Chapter 5 List of Tables.....	i
Chapter 5 List of Figures .....	ii
Executive summary .....	243
Chapter 5.    AQUIFER CAPACITY IN SANA'A BASIN .....	243
General Outline .....	244
5.1          Characteristics of the Pumped Wells .....	245
5.2          Hydraulic parameters of the alluvium aquifer .....	246
5.2.1      Methodology for analysis of large-diameter pumped wells .....	248
5.2.2      Method of analysis used for multi-step test .....	250
5.2.3      Interpretation of the results of pumping and step tests .....	250
5.2.4      Spatial distribution of alluvium aquifer constants .....	260
5.3          Hydraulic characteristics of the volcanic aquifer .....	269
5.3.1      Analysis method for small-diameter pumped wells (Cooper-Jacob method) .....	269
5.3.2      Cooper-Jacob Time-Drawdown method .....	271
5.3.3      Interpretation of the results of the new pumping tests .....	271
5.3.4      Interpretation of the results of the pumping tests on record .....	274
5.3.5      Spatial distribution of volcanic aquifer constants .....	276
5.4          Hydraulic characteristics of the Tawilah sandstone aquifer .....	280
5.4.1      Analysis method for small-diameter pumped wells (Cooper-Jacob method) .....	280
5.4.2      Interpretation of results of the new pumping tests .....	282
5.4.3      Interpretation of results of re-analyzed pumping tests .....	285
5.4.4      Spatial distribution of Tawilah sandstone aquifer constants .....	296
5.5          Conclusions .....	302

## CHAPTER 5 LIST OF TABLES

Table 5-1	Wells in the study area classified by well diameter .....	245
Table 5-2	Means of water lifting.....	245
Table 5-3	Number of wells in each aquifer type .....	246
Table 5-4	Alluvium aquifer parameters estimated from pumping and recovery tests in Sana'a Basin (Feb. 2007).....	259
Table 5-5	Results of step drawdown test in well no. HAS 5.....	268
Table 5-6	Results of step drawdown test in well no. HSA 19.....	269
Table 5-7	Estimated values of formation loss, well loss and laminar flow ratio of the alluvium aquifer in Sana'a Basin.....	269
Table 5-8	Results of the long-duration pumping test carried out in the volcanic aquifer wells in Bani Matar, Sana'a Basin .....	271

Table 5-9	Results of the step drawdown test in wells EX-1 and EXP-2 of the volcanic aquifer in Bani Matar, Sana'a Basin .....	272
Table 5-10	Results of new pumping tests and tests on record carried out in the volcanic aquifer wells in Sana'a Basin.....	275
Table 5-11	Results of new pumping and recovery tests carried out in deep wells of Tawilah sandstone aquifer applying the Cooper-Jacob method (Dec.2006) .....	285
Table 5-12	Errors committed on previous interpretation of pumping tests on record .....	286
Table 5-13	Description of graphs obtained from re-analysis of past pumping test data from Tawilah sandstone deep wells in Sana'a Basin .....	291
Table 5-14	Comparison between the re-analyzed pumping tests results and the past results ...	293
Table 5-15	P probable causes of difference between calculated transmissivity from pumping and recovery tests for some selected re-analyzed pumping test data in Tawilah sandstone aquifer wells in Sana'a Basin .....	295
Table 5-16	Ranges of calculated transmissivity values in re-analysed pumping tests of Tawilah sandstone aquifer wells in Sana'a Basin (Total number of wells = 81).....	296
Table 5-17	Ranges of aquifer potential (Zekai Sen, 1995).....	297
Table 5-18	Results of estimated storage coefficient in the Tawilah sandstone aquifer in Sana'a Basin .....	297

## CHAPTER 5 LIST OF FIGURES

Figure 5-1	Spatial distribution map of the selected pumping tests in dug wells.....	248
Figure 5-2	Family of type curves according to Papadopulos-Cooper 1967 .....	249
Figure 5-3	Preparation of pumping test in well HSA36 (upper), measuring well discharge in m <sup>3</sup> /min (middle photo) and recovery from fractures (lower photo) .....	251
Figure 5-4	Matching of time-drawdown data of large diameter well with Papadopulos-Cooper type curve (well no. HSA 62 - Bani El-Hareth) .....	252
Figure 5-5	Matching of time-drawdown data of large diameter well with Papadopulos-Cooper type curve (well no. HSZ 12 - Bani Mattar).....	252
Figure 5-6	Matching of time-drawdown data of large diameter well with Papadopulos-Cooper type curve (well no. HSA 61- Bani El-Hareth) .....	253
Figure 5-7	Matching of time-drawdown data of large diameter well with Papadopulos-Cooper type curve (well no. HSA 54 - Bani El-Hareth) .....	253
Figure 5-8	Matching of time-drawdown data of large diameter well with Papadopulos-Cooper type curve (well no. HSA 55).....	254
Figure 5-9	Matching of time-drawdown data of large diameter well with Papadopulos-Cooper type curve (well no. HS 70).....	255
Figure 5-10	Matching of time-drawdown data of large diameter well with Papadopulos-Cooper type curve (well no. HS 66).....	255
Figure 5-11	Matching of time-drawdown data of large diameter well with Papadopulos-Cooper type curve (well no. HSA19).....	256
Figure 5-12	Matching of time-drawdown data of large diameter well with Papadopulos-Cooper type curve (well no. HSA 26).....	256
Figure 5-13	Matching of time-drawdown data of large diameter well with Papadopulos-Cooper type curve (well no. HSA 30).....	257

Figure 5-14	Matching of time-drawdown data of large diameter well with Papadopulos-Cooper type curve (well no. HSA 31).....	257
Figure 5-15	Matching of time-drawdown data of large diameter well with Papadopulos-Cooper type curve (well no. HS 51).....	258
Figure 5-16	Matching of time-drawdown data of large diameter well with Papadopulos-Cooper type curve (well no. HSA 36).....	258
Figure 5-17	Matching of time-drawdown data of large diameter well with Papadopulos-Cooper type curve (well no. HSs 3).....	259
Figure 5-18	Hydraulic conductivity distribution zonation map of the alluvium aquifer in Sana'a Basin.....	262
Figure 5-19	Transmissivity distribution zonation map of the alluvium aquifer in Sana'a Basin....	263
Figure 5-20	Specific yield distribution zonation map of the alluvium aquifer in Sana'a Basin.....	264
Figure 5-21	Figure 5- 20 The weak inverse relationship between transmissivity ( $m^2/d$ ) and specific yield (dimensionless) of the alluvium aquifer.....	265
Figure 5-22	Figure 5- 21 The moderate inverse relationship between transmissivity and total depth of the pumped well in alluvium aquifer .....	265
Figure 5-23	Figure 5- 22 The general trend between the total drawdown (m), the residual drawdown (m) and the discharge ( $m^3/d$ ) from the wells tested in the alluvium aquifer .....	266
Figure 5-24	Figure 5- 23 The general trend between the pumping duration (h) and the total drawdown (m) in the wells tested in the alluvium aquifer .....	266
Figure 5-25	Figure 5- 24 The general trend between the recovery duration (h) and the residual drawdown (m) in the wells tested in the alluvium aquifer.....	267
Figure 5-26	Figure 5- 25 The result of the step test carried out in well no. HSA 5, Bani El-Hareth.....	268
Figure 5-27	Figure 5- 26 The result of the step test carried out in well no. HSA19, Bani El-Hareth.....	268
Figure 5-28	Figure 5- 27 Graph showing the conditions appropriate to the solution of Cooper-Jacob method .....	270
Figure 5-29	Figure 5-28 The graphical solution of the long-duration pumping and recovery test carried out on well EXP-1 in the volcanic aquifer in Sana'a Basin (May 2006).....	273
Figure 5-30	Figure 5-29 The graphical solution of the long-duration pumping and recovery test carried out on well EXP-2 in the volcanic aquifer in Sana'a Basin (June 2007).....	274
Figure 5-31	Figure 5- 30 The relationship between the estimated K values from pumping tests and from transmissivity values of volcanic aquifer in Sana'a Basin.....	277
Figure 5-32	Figure 5- 31 The spatial distribution map of the hydraulic conductivity of the volcanic aquifer in Sana'a Basin .....	278
Figure 5-33	Figure 5- 32 The spatial distribution map of the transmissivity of the volcanic aquifer in Sana'a Basin .....	279
Figure 5-34	Figure 5- 33 The location map of the newly pumped wells and re-analyzed wells...	281
Figure 5-35	Figure 5- 34 The graphical solution of the pumping and recovery test carried out on well HS-50 in Tawilah sandstone aquifer in Sana'a Basin (Dec. 2006) .....	282
Figure 5-36	Figure 5- 35 The graphical solution of the pumping and recovery test carried out on well HS-56 in Tawilah sandstone aquifer in Sana'a Basin (Dec. 2006) .....	283

Figure 5-37	Figure 5- 36 The graphical solution of the pumping and recovery test carried out on well HS-63 in Tawilah sandstone aquifer in Sana'a Basin (Jan. 2007).....	284
Figure 5-38	Figure 5- 37 The graphical solution of the recovery test carried out on well HS-55 in Tawilah sandstone aquifer in Sana'a Basin (Dec 2006).....	285
Figure 5-39	Figure 5- 38 <b>Hydraulic conductivity distribution</b> zonation map of the Tawilah sandstone aquifer in Sana'a Basin .....	299
Figure 5-40	Figure 5- 39 Transmissivity distribution zonation map of the Tawilah sandstone aquifer in Sana'a Basin .....	300
Figure 5-41	Figure 5- 40 Storage coefficient distribution zonation map of theTawilah sandstone aquifer in Sana'a Basin .....	301

## Chapter 5. AQUIFER CAPACITY IN SANA'A BASIN

### EXECUTIVE SUMMARY

The aquifer's capacity to store groundwater is determined using parameters derived from pumping tests. The results of new tests and re-analyzed tests are described in this chapter:

- In the alluvial aquifer: 14 constant discharge and 2 multi-step tests;
- In the volcanic aquifer: 2 constant discharge and 2 multi-step tests; also 20 tests on record were re-analyzed;
- In the sandstone aquifer: 3 constant discharge and 4 recovery tests; also 45 tests on record were re-analyzed.

	Number of wells	Hydraulic Conductivity (m/d)			
		Min	Avg	Max	Method
Alluvium	14	0.09	1.75	12.23	Papadopulos and Cooper
Volcanic	22	0.0004	0.09	0.42	Cooper-Jacob (old tests)
Sandstone	81	0.5	7.3		Cooper-Jacob (old tests)

	Number of wells	Transmissivity (m <sup>2</sup> /d)			
		Min	Avg	Max	Method
Alluvium	14	9	511	3,618	Papadopulos and Cooper
Volcanic	22	0.34	47	200	Cooper-Jacob (new tests)
Sandstone	4	23.5	81.5	148	Cooper-Jacob (new tests)
	81	6	170	3770	Cooper-Jacob (old tests)

	Number of wells	Specific Yield			
		Min	Avg	Max	Method
Alluvium	14	0.0004	0.0096	0.078	Papadopulos and Cooper

	Number of wells	Storage Coefficient			
		Min	Avg	Max	Method
Sandstone	4	0.41x10 <sup>-4</sup>	4.1x10 <sup>-4</sup>	9.6x10 <sup>-4</sup>	Cooper-Jacob (new tests)
	81	1.5x10 <sup>-4</sup>	2.2x10 <sup>-3</sup>	9.4x10 <sup>-3</sup>	Cooper-Jacob (old tests)

The tests in the alluvium indicate unconfined conditions. The range in conductivity values is large. The higher values are found in the northern (thicker) part of the aquifer. The low specific yield of this aquifer indicates the effect of clays and silts within the alluvial deposits.

The tests in the volcanic aquifer reflect the low regional conductivity and the high local conductivity, the latter caused by weathering or fracturing. This results in a large range of hydraulic conductivity values. The storage coefficient of the volcanic aquifer was not analyzed.

The tests in the Tawilah sandstone also reflect the effect of fracturing. More conclusions on the tests in the sandstone aquifer can be found at the end of this chapter.

## GENERAL OUTLINE

In the Sana'a Basin, an approximate number of 11,600 wells can be found (WEC, 2001). The wells are roughly divided into three groups according to their construction:

- Dug wells;
- Drilled wells, cased only in unconsolidated sediment and uncased in underlying hardrock;
- Drilled wells, cased over the total well depth and screened near the bottom of the well.

Dug wells (type 1) are dug into the Alluvium to about 5 metres below groundwater level and have diameters of 1.5 to 3 m. The casing of the dug wells consists of stones which are cemented against the wall or concrete tubes (1.5 m diameter and 1 m length) which are stacked on top of each other. This type of casing is not waterproof when saturated; water can flow through cracks where cementing is not one hundred percent. The design of the drilled wells is based on the expected geology of the subsurface and the amount of money the future owner is willing to pay for the well. The price of the well depends mainly on the amount and type of casing. The most common type of casing used in the Sana'a Basin is carbon steel casing. The casing consists of 6 m-length carbon steel pipes with diameters of 16, 14 or 12 inches. The type of screen used is made of the same metal as the casing.

For well type 2, the drilling pipes are removed when the drilling has entered the hardrock for some meters and the casing is installed over the whole depth of the borehole. The pipes are not cemented at the bottom of the hole but are forced into the hardrock. After installation of the casing, the annular space is filled with gravel pack. Drilling proceeds with a smaller diameter until the required depth of the well. This type of well can be found in areas where alluvium covers hardrock, such as Tertiary basalts or Tawilah sandstone, which are not prone to collapse. No screen is added to the casing in the alluvium because of the risk of contamination.

For well type 3, drilling proceeds until the required depth of the well and the casing is entered until the bottom of the well. The deepest part of the casing consists of a screen with a length varying from 24-150 m. This type of well can be found in areas where Quaternary volcanics **inter-fingers** with alluvium or Amran limestone. Both rock types are prone to collapse.

Good management of water resources in any area requires a good knowledge of the aquifer capacity. Pumping tests are a vital tool for estimating aquifer capacity. During pumping, water levels go down in the pumped well and in surrounding observation wells. The difference between the original water level (static water level) and the water level during pumping (dynamic water level) is called drawdown.

The form of the time-drawdown curve is affected by a number of different factors. The most important ones are:

1. Storage of water inside the well,
2. Degree of hydraulic contact between the well and the aquifer, which depends on:
  - Length of well screen or well face in relation to aquifer thickness (penetration ratio),
  - Hydraulic characteristics of the aquifer (e.g. transmissivity, storage coefficient, anisotropy),
  - Spatial variation of hydraulic aquifer characteristics,
  - Aquifer limits (negative boundaries) and recharge boundaries (positive boundaries),
  - Variation of well discharge.

A drawdown test (during which drawdown increases in time) can be followed by a recovery test. During a recovery test, the decrease of drawdown in time is measured starting from the moment the pump is shut down. Interpretation of drawdown and recovery tests for the determination of hydraulic aquifer parameters follows a systematic sequence of steps:

- Select the most appropriate model,
- Determine visually which part of the field curve should correspond to this model,
- Match that part of the curve to the selected model by any adequate graphical or numerical method available and determine the aquifer parameters(s) according to a standard method,
- Judge whether the matching and the obtained parameter values confirm the selected model, if not, go back to step 1, select another model and repeat the procedure.

The selection of the model is usually the most critical step. The aquifer capacity in Sana'a Basin was discussed for three aquifers: the Quaternary alluvium aquifer, the Tawilah Cretaceous sandstone aquifer and the Tertiary volcanic aquifer. A brief discussion of the estimated hydraulic characteristics of these follows.

### 5.1 Characteristics of the Pumped Wells

During the field work related to the determination of aquifer capacity (Dec. 2006-Feb. 2007), well characteristics such as well diameter, water lifting method and number of wells in each surveyed aquifer were classified and tabulated. Table 5-1 indicates that there are 100 large-diameter wells (greater than 1 m), while there are 73 wells with a diameter less than 1 m.

**Table 5-1 Wells in the study area classified by well diameter**

Type of wells	Well Diameter (m)							
	0.20- 0.25	0.25- 0.30	0.30 - 0.35	0.35 - 0.50	0.50 - 1	1 -1.50	1.50 -2.0	>2.0
Dug	0	0	0	0	0	2	89	9
Dug/Bore	0	2	0	5	0	0	0	0
Bore	7	34	0	24	1	0	0	0
Total	7	36	0	29	1	2	89	9

With respect to water-lifting methods from the productive well, out of 37 wells, 35 wells (or 95%) do so by mechanical means, as shown in Table 5-2. Three different types of pumps are installed, most common of which is Caprari. As for engines, there are four different types of engines and the most common is Yanmar.

**Table 5-2 Means of water lifting**

Water Lifting device	Number of wells
Motorized pump	33
Submersible pump	2

Water Lifting device	Number of wells
House pump	0
Bucket	2
Total	37

There are three main aquifer types in the Sana'a Basin: alluvium aquifer with 38% of the total number of monitored wells, Tawilah sandstone aquifer with 37.5% of the monitored wells, and the volcanic aquifer with 5% of the monitored wells. The remaining monitored wells are located within the Amran limestone group. With respect to the type of wells in each aquifer, a significant variation has been observed. For dug wells, 53% of them are in the alluvium aquifer, 20% in the Tawilah sandstone aquifer, 5% in the volcanic aquifer and the rest in the Amran limestone group. For boreholes, 18% of them are in the alluvium aquifer, 59% in the Tawilah sandstone aquifer, 6% in the volcanic aquifer and the rest in the Amran limestone group. Thus, almost half the dug wells are in an alluvium aquifer, while half of the drilled ones are in a Tawilah sandstone aquifer, as indicated in Table 5-3.

**Table 5-3 Number of wells in each aquifer type**

Type of well	Aquifer type				Total
	A	V	S.S	L.S	
Dug	49	5	19	20	93
Dug/Bore	3	0	4	0	7
Boreholes	12	4	40	12	68
Total	64	9	63	32	168

A: alluvium aquifer; S.S: Tawilah sandstone aquifer; V: volcanic aquifer; L.S: Amran limestone group

## 5.2 Hydraulic parameters of the alluvium aquifer

The unconsolidated deposits of the Quaternary cover reach 15% of the basin area. They are confined to wadi beds and low areas that form the Sana'a Plain. Deposition appears to have been of a fluvio-lacustrine nature, which led to the accumulation of clays and silts in basins of 100 m to 300 m deep. Coarse-grained alluvium deposits occur in the wadi beds at the foot of hills. The sedimentary sequence is block-faulted and gently folded. The regional dip is southwards under cover of the Tertiary volcanic group. The unconsolidated Quaternary deposits provide a poorly permeable aquifer which has been heavily exploited in the Sana'a Basin due to urbanization activities. The aquifer is regionally unconfined but locally semi-confined. Due to the fine-grained nature of the deposits in the plain, recharge is expected to be mainly indirect, into coarse-grained material along wadis and at the base of the hills.

Hydraulic parameters include transmissivity (T), hydraulic conductivity (K), and storativity (S) or specific yield in case of unconfined aquifer. These parameters reflect the ability of the aquifer for transmitting, storing and yielding groundwater. They also play an important role in the recharge rates from and to the aquifer. Due to the importance of these parameters, many tests are carried out to determine the hydraulic parameters of alluvium aquifer.



In many parts of Sana'a Basin, large-diameter dug wells partially penetrate the alluvium aquifer. These wells are generally available for carrying out aquifer tests. Among 49 of surveyed dug wells, 17 dug wells were chosen for testing the hydraulic characteristics of the Alluvium aquifer. The selection was based on acceptance of the owners to carry out the test, productivity of the dug well, water column length inside the dug well and spatial distribution of these wells to cover the aquifer. The spatial distribution of these wells is given in Figure 5-1.

When pumping is done from such wells, the various methods of Theis, based on the assumption that the well radius is small and that all the water is released from storage in the aquifer, are not applicable as water stored in the well contributes a significant proportion of well discharge. Information with regard to lithology and the observed water levels suggest that the Quaternary alluvium aquifer is likely to behave as a non-leaky unconfined aquifer.

Typical drawdown curves for pump tests in an unconfined aquifer are present in Kreuzman and De Ridder 1990. Characteristic for such curves is an intermediate trajectory showing an approximately constant drawdown during a certain lapse of time. Responsible for this phenomenon is the so-called 'delayed gravity response' effect: early drawdown is governed by elastic storage (like in a confined aquifer), whereas the drainage of pores near the water table becomes effective only after some time and constitutes the dominant storage depletion mechanism at later times (Skibitzke, H.E. 1958). It is convenient to divide the drawdown curves correspondingly into type curves of early times and type curves of later times.

Some special factors should be taken into account:

- **Partial penetration:** all the wells tested partially penetrate the exploited aquifer with unknown penetration ratio,
- **Well-bore storage** affects drawdown at the beginning of both the drawdown and recovery tests, except for the wells experiencing complete storage depletion.

Hydraulic 'well entry losses' are likely to occur in screened and cased wells (most dug wells, however, are unlined below the water table).

No analytical models are available as yet that incorporate all factors mentioned above. The model that comes closest to this condition is the Papadopulos and Cooper model (1967) for large-diameter, partially-penetrating wells in an unconfined aquifer. This model includes well-bore storage effects and can be used to describe the initial field curves.

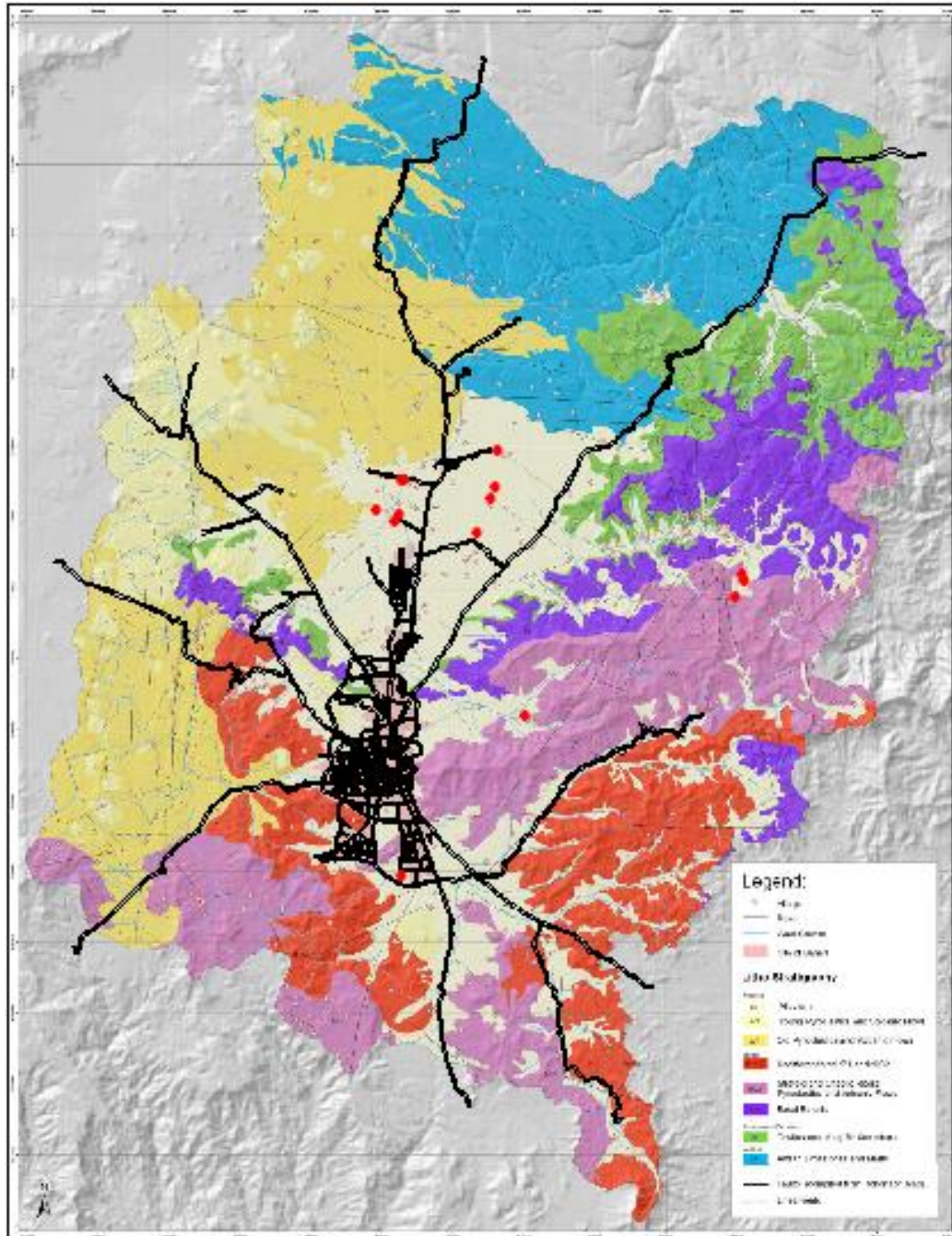


**Figure 5-1 Spatial distribution map of the selected pumping tests in dug wells**

### 5.2.1 Methodology for analysis of large-diameter pumped wells

One method for analyzing pump test data of large-diameter wells cased to the top of an extensive artesian (or unconfined) aquifer and screened (or open) throughout the thickness of the aquifer, taking into account the storage capacity of the well, was presented by Papadopoulos and Cooper (1967, p. 244). The assumptions made are the same as in the Theis method, except for the diameter of the well. The equation applicable for flow into a well of large diameter is:

$$s = \frac{Q \times F(u_w, \alpha)}{4 \pi T}$$

where:

**Q** = constant discharge (m<sup>3</sup>/d)

**s** = drawdown in the well (m)

**T** = transmissivity (m<sup>2</sup>/d)

**F(u<sub>w</sub>, α)** is a function

$$u_w = \frac{r_w^2 \times S}{4 T t}$$

$$\alpha = \frac{r_w^2 \times S}{r_c^2}$$

where:

**r<sub>c</sub>** = radius of the unscreened part of the well (m)

**r<sub>w</sub>** = radius of the screened part of the well (m)

**t** = time since pumping started (d)

**S** = storativity or specific yield (dimensionless)

The method involves preparation on logarithmic paper of a family of type curves **F(u<sub>w</sub>, α)** versus **1/u<sub>w</sub>** for different values of **α** (Figure 5-2).

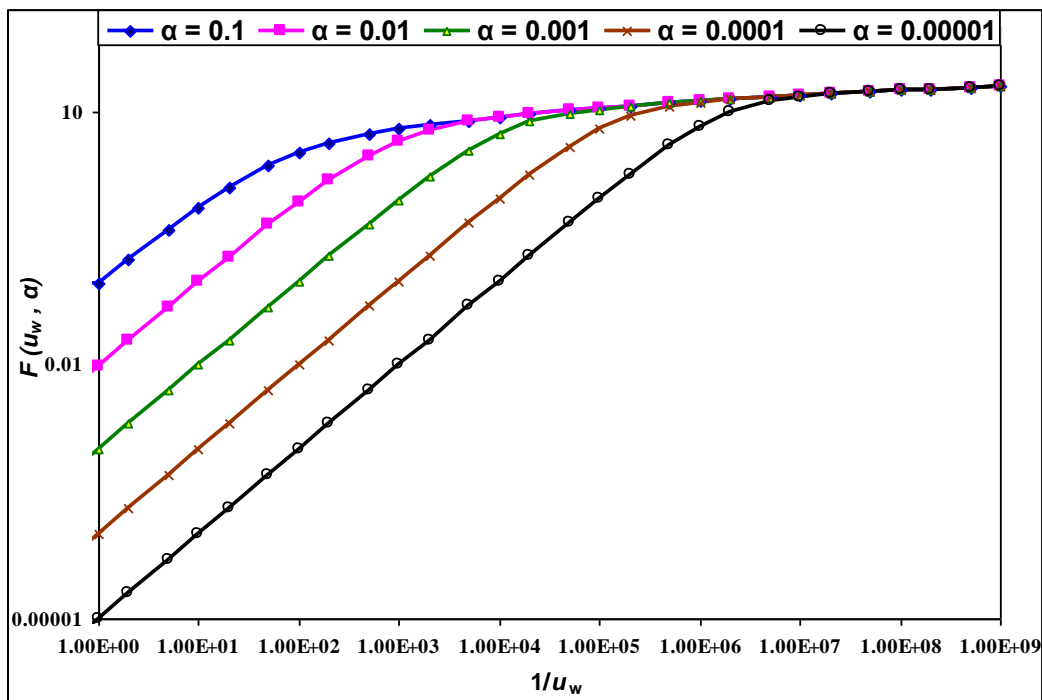


**Figure 5-2 Family of type curves according to Papadopoulos-Cooper 1967**

The time-drawdown data of the pumped well are plotted separately on logarithmic paper of the same scale as the type curve, super-imposed on the type curve and adjusted to a position that best fits one of the type curves. An arbitrary point is selected and the values of **F(u<sub>w</sub>, α)**, **1/u<sub>w</sub>**, **s**, **t**, as well as the value of **α** of the matched type curve, are read. The value of **s** and **F(u<sub>w</sub>, α)** read from the graphs and accordingly the estimated values of **T** and **S** is calculated.

### 5.2.2 Method of analysis used for multi-step test

The drawdown in a well due to withdrawal of water is usually made up of head loss resulting from laminar flow in the formation (formation loss), and head loss resulting from turbulent flow in the zone close to the well face, through the well screen and well casing (well loss). The data of these tests were analyzed by application of an empirical formula (Walton, 1962) and the well losses in these wells were calculated based on the method given by (Jacob, 1946):

$$s_w = BQ + CQ^2$$

$$s_w / Q = B + CQ$$

where

$s_w$  : well drawdown (m)

$C$  : well loss coefficient ( $\text{min}^2/\text{m}^5$ )

$B$  : formation loss coefficient ( $\text{h}/\text{m}^2$ )

$Q$  : discharge ( $\text{m}^3/\text{min}$ )

$s_w/Q$  : the specific drawdown of the well

The drawdown in a pumped well ( $s_w$ ), is the summation of drawdown due to formation loss ( $BQ$ ), and drawdown due to well loss ( $CQ^2$ ).

Plotting the specific drawdown against discharge for several steps, the well loss and the formation loss coefficients were determined from the slope and intercept of the straight line plots respectively.

### 5.2.3 Interpretation of the results of pumping and step tests

During the field activities, the alluvium aquifer was tested through 14 constant discharge pumping tests for productive wells no. **HSA 62, HSZ 12, HSA 61, HSA 54, HSA 55, HS 70, HS 66, HSA19, HSA 26, HSA 30, HSA 31, HS 51, HSA 36** and **HSs 3** in Bani Husheish, Bani Al-Harith, Bani Matar and Sa'awan areas. While the two multi-step tests were carried out on wells no. **HSA 5** and **HSA 19** (Figure 5-1).

The field data of these pumping tests were analyzed applying Papadopoulos and Cooper model (1967) and their results are shown in Figures 5-3 to 5-16. The hydraulic parameters of the alluvium aquifer are given in Table 5-4.



**Figure 5-3** Preparation of pumping test in well HSA36 (upper), measuring well discharge in  $\text{m}^3/\text{min}$  (middle photo) and recovery from fractures (lower photo)

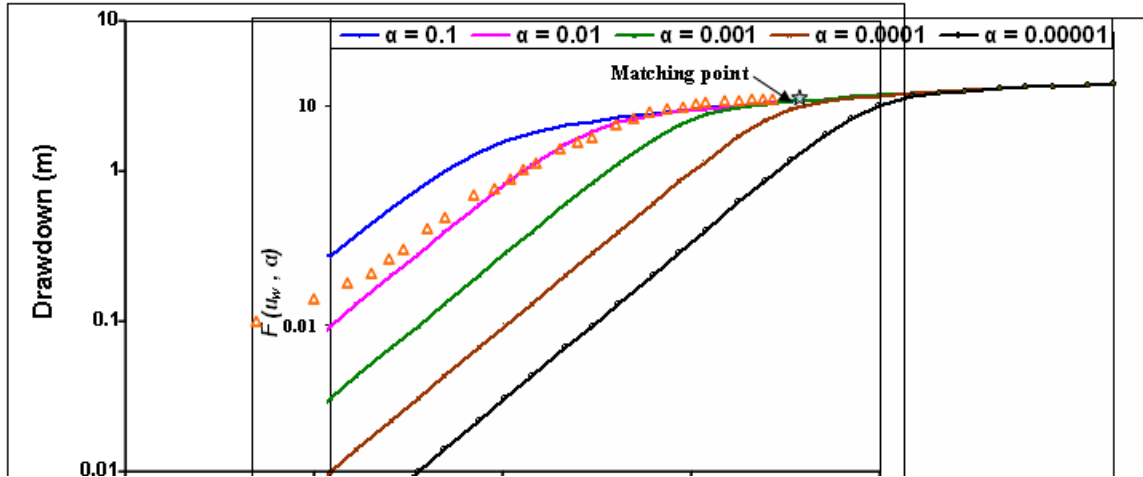


**Figure 5-4** Matching of time-drawdown data of large diameter well with Papadopolos-Cooper type curve (well no. HSA 62 - Bani El-Hareth)

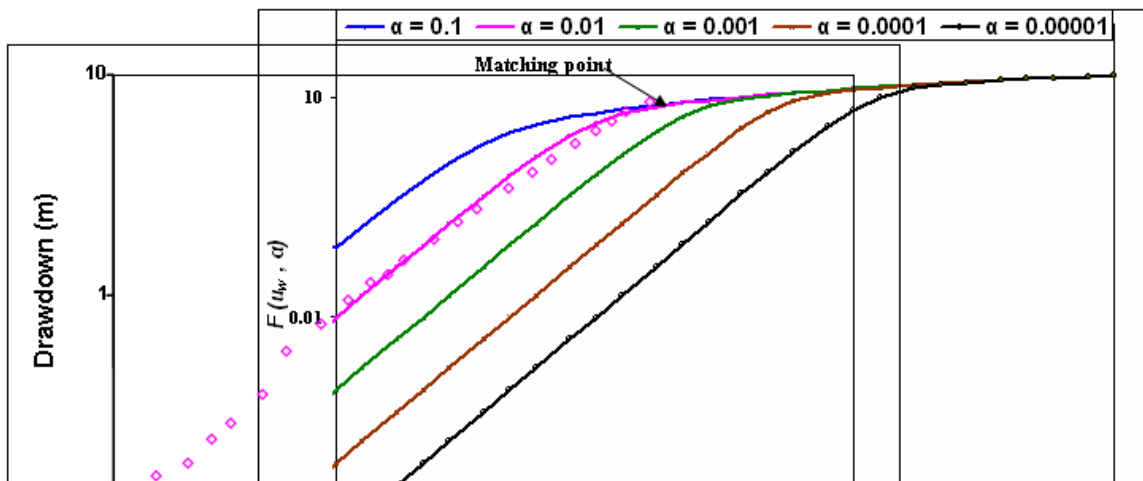


**Figure 5-5** Matching of time-drawdown data of large diameter well with Papadopolos-Cooper type curve (well no. HSZ 12 - Bani Mattar)

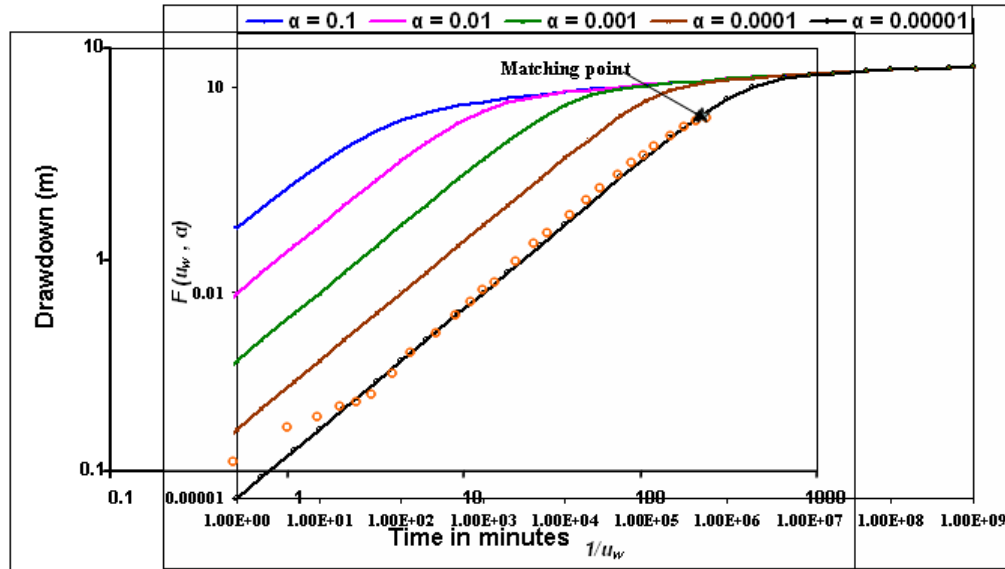


**Figure 5-6** Matching of time-drawdown data of large diameter well with Papadopulos-Cooper type curve (well no. HSA 61- Bani El-Hareth)

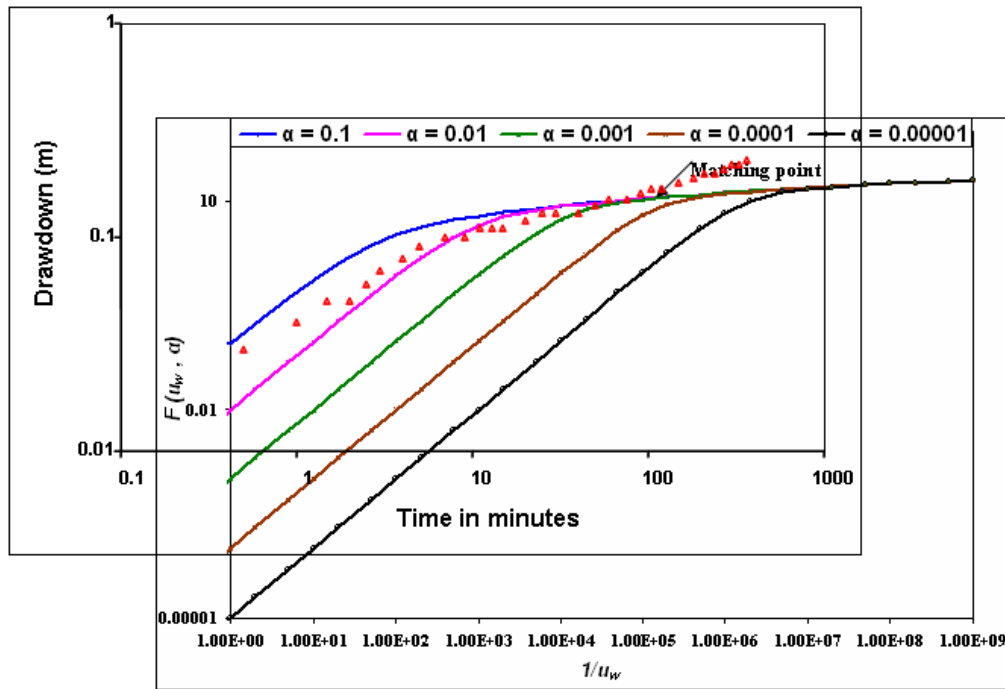


**Figure 5-7** Matching of time-drawdown data of large diameter well with Papadopulos-Cooper type curve (well no. HSA 54 - Bani El-Hareth)

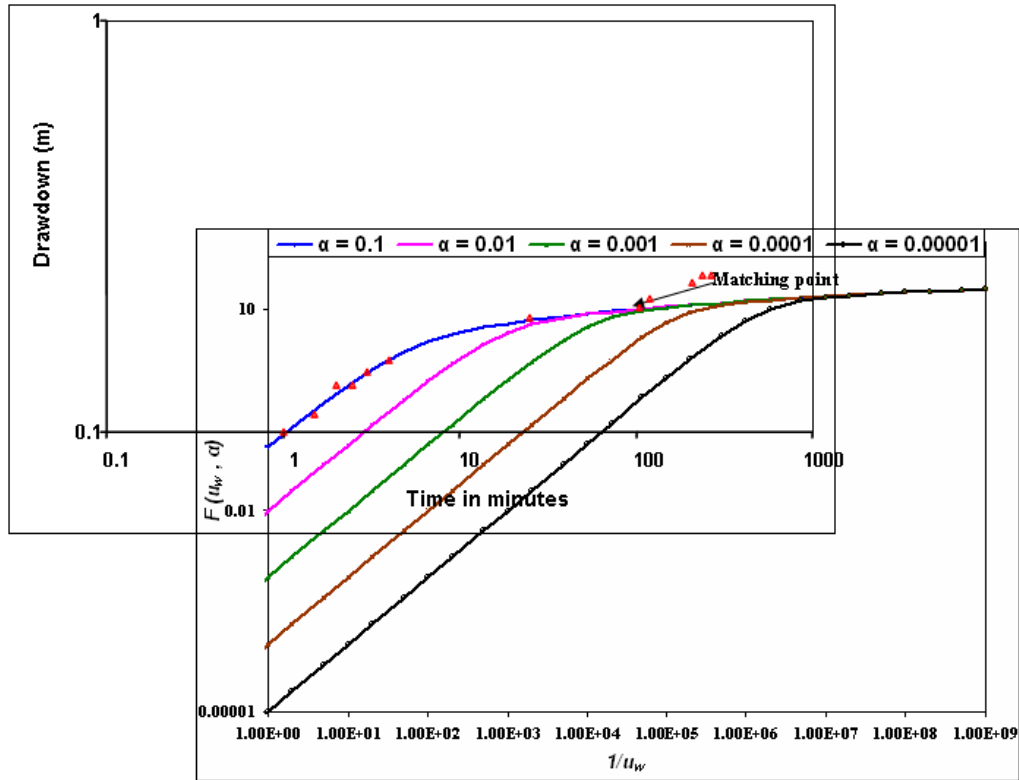


**Figure 5-8 Matching of time-drawdown data of large diameter well with Papadopulos-Cooper type curve (well no. HSA 55)**



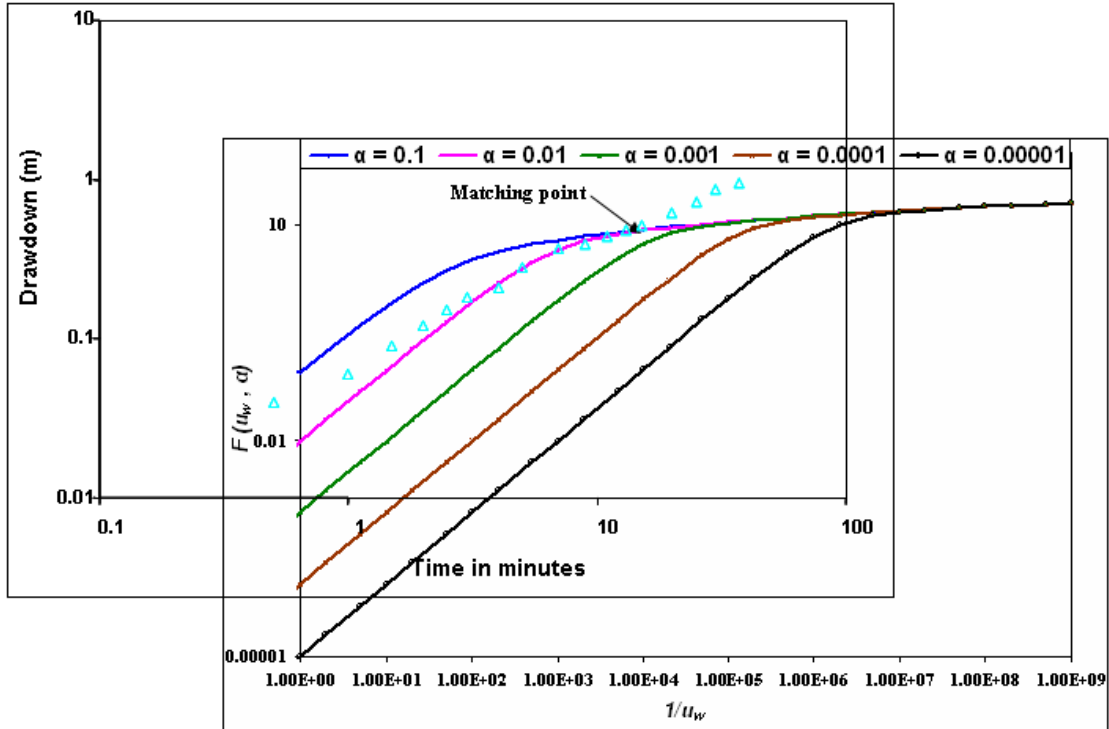


**Figure 5-9** Matching of time-drawdown data of large diameter well with Papadopolos-Cooper type curve (well no. HS 70)

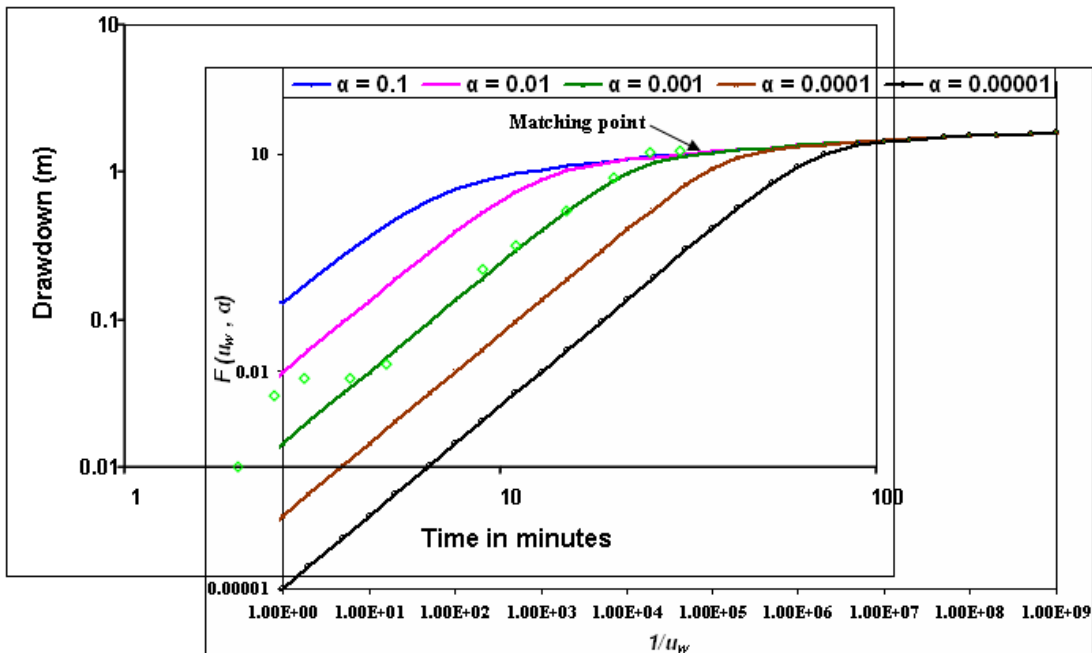


**Figure 5-10** Matching of time-drawdown data of large diameter well with Papadopolos-Cooper type curve (well no. HS 66)

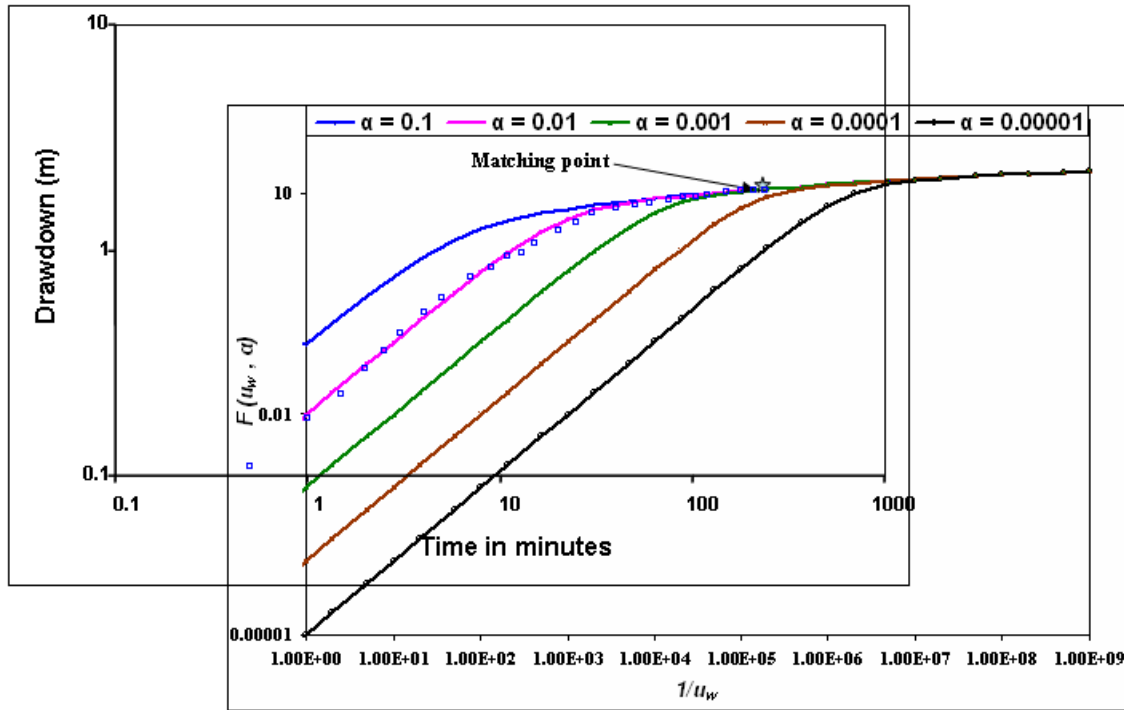


**Figure 5-11** Matching of time-drawdown data of large diameter well with Papadopolus-Cooper type curve (well no. HSA19)

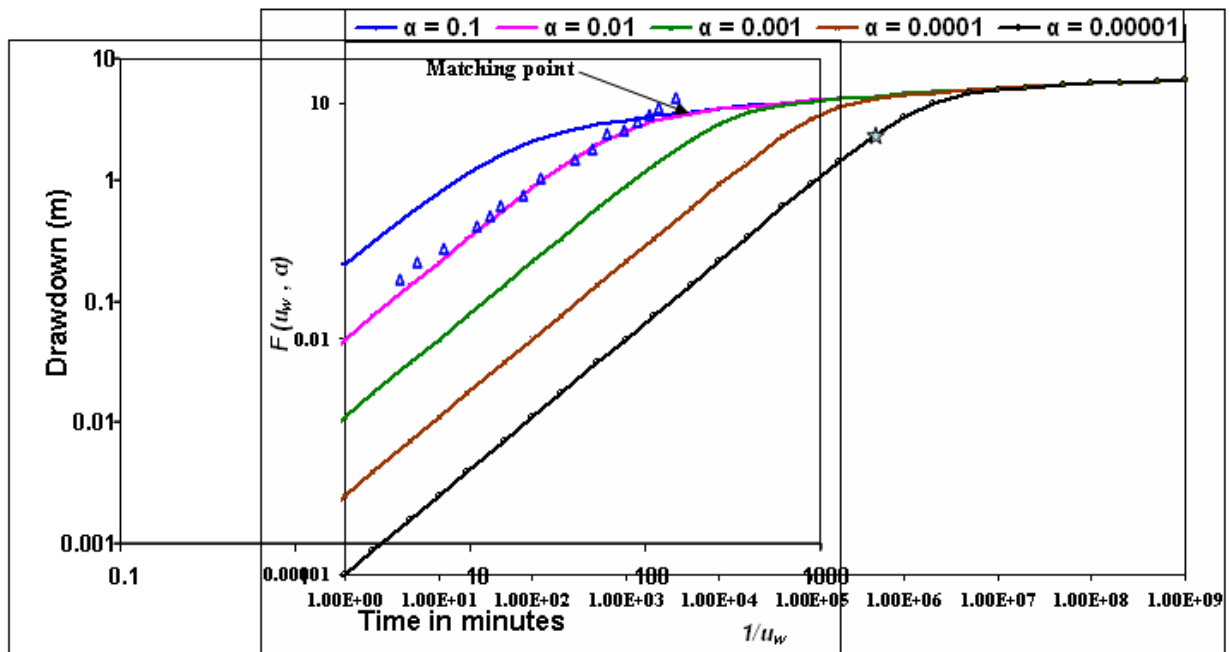


**Figure 5-12** Matching of time-drawdown data of large diameter well with Papadopolus-Cooper type curve (well no. HSA 26)

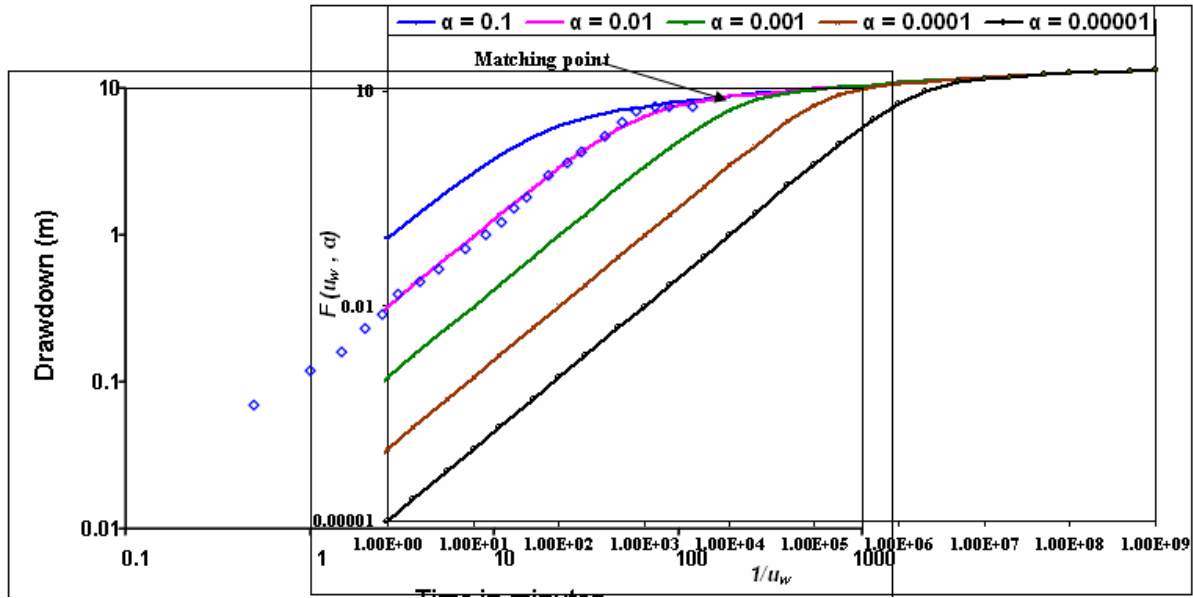


**Figure 5-13** Matching of time-drawdown data of large diameter well with Papadopolus-Cooper type curve (well no. HSA 30)

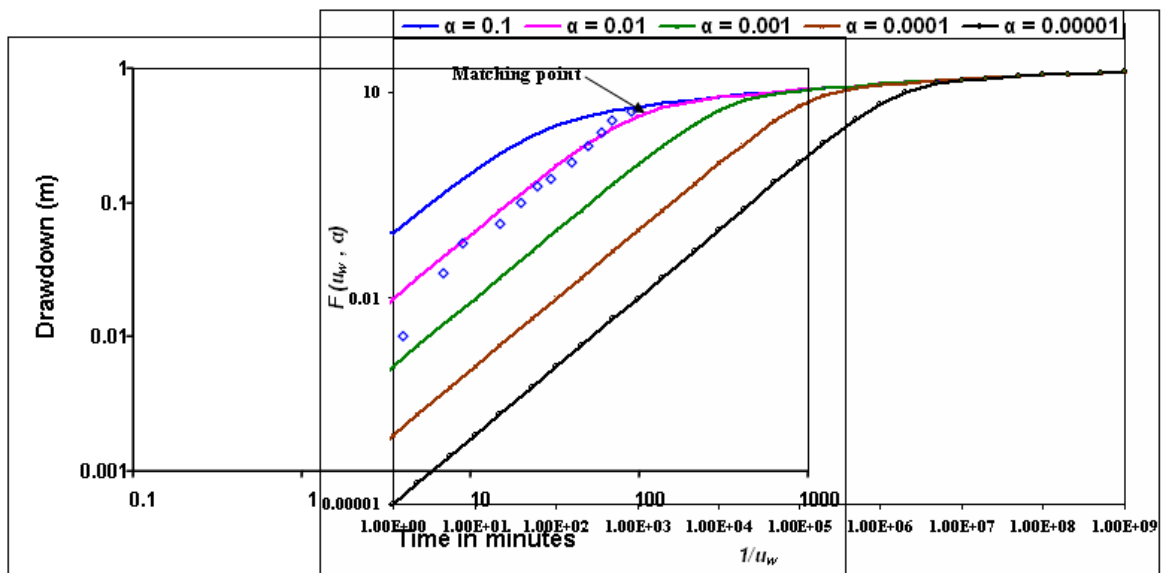


**Figure 5-14** Matching of time-drawdown data of large diameter well with Papadopolus-Cooper type curve (well no. HSA 31)

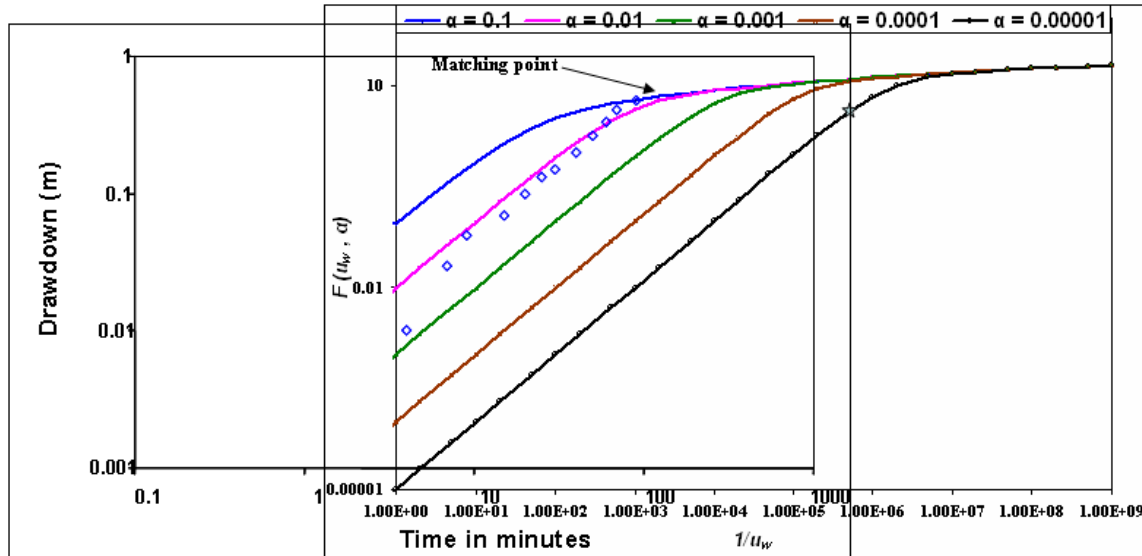


**Figure 5-15** Matching of time-drawdown data of large diameter well with Papadopulos-Cooper type curve (well no. HS 51)

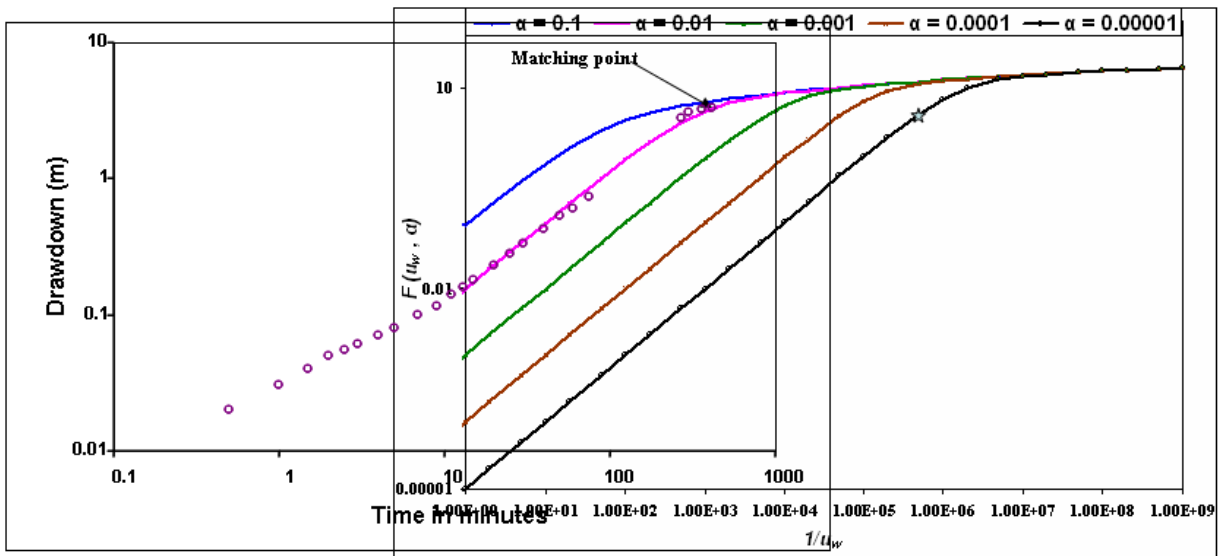


**Figure 5-16** Matching of time-drawdown data of large diameter well with Papadopulos-Cooper type curve (well no. HSA 36)

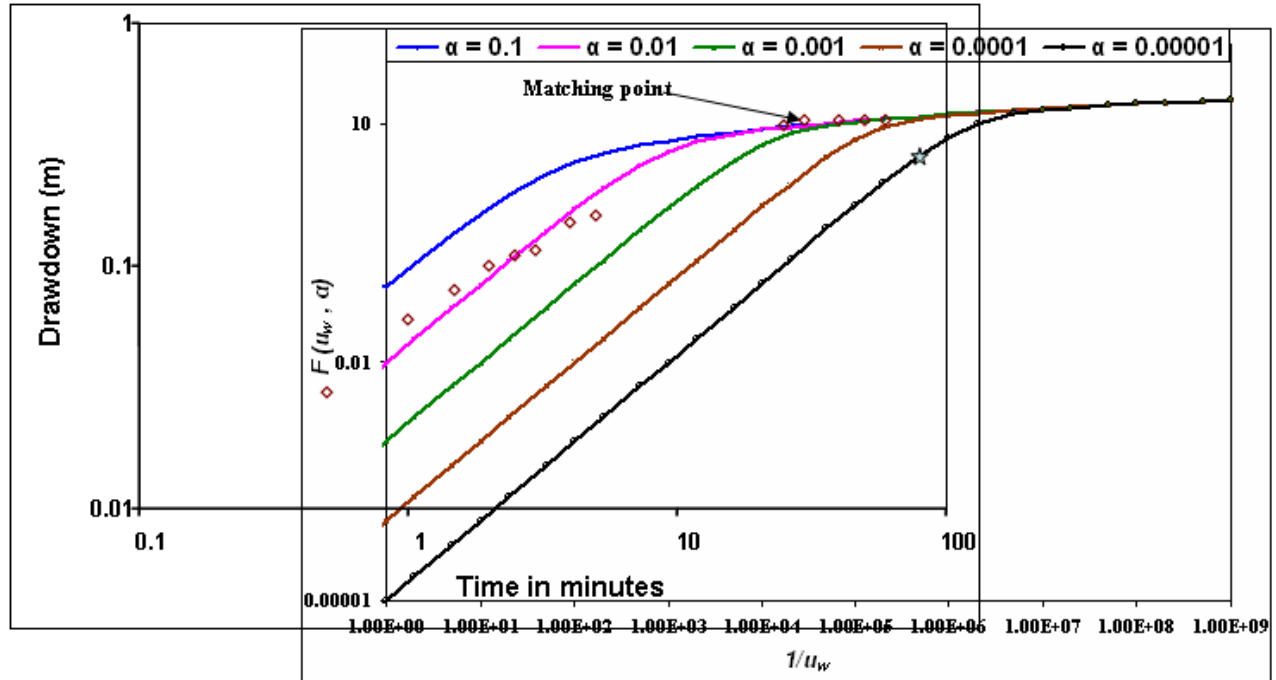


**Figure 5-17** Matching of time-drawdown data of large diameter well with Papadopulos-Cooper type curve (well no. HSs 3)

**Table 5-4** Alluvium aquifer parameters estimated from pumping and recovery tests in Sana'a Basin (Feb. 2007)

S.N	Well ID	TD (m)	DTW (m)	Q (m <sup>3</sup> /h)	PD (h)	TDD (m)	RD (h)	RDD (m)	T (m <sup>2</sup> /d)	K (m/d)	Sy
1	HS 51	30	27.7	294	1.33	6.29	2.75	1.7	25	1.33	0.008
2	HS 70	39	7.72	365	0.62	0.94	2.5	0.26	472	0.84	0.0013
3	HS 66	31	26.5	432	0.5	1.38	2	0.02	241	0.15	0.0004
4	HSA19	55	52.7	432	4	1.85	0.98	0.51	202	0.21	0.00135
5	HSA26	33	33	132	5.5	10.26	1.75	1.71	30	0.52	0.001
6	HSA30	50	21.5	370	2	7.46	2.5	0.1	33	0.12	0.0011
7	HSA31	70	25	74	1.5	0.47	5	1.39	76	1.11	0.009
8	HSA36	120	49.1	58	7	3.27	4	0.22	9	12.23	0.0087
9	HSs 3	30	27.1	200	1	0.4	6	2.29	336	6.58	0.0033
10	HSA54	33	28.3	458	6	0.23	5	0.29	3618	0.61	0.00049

S.N	Well ID	TD (m)	DTW (m)	Q (m <sup>3</sup> /h)	PD (h)	TDD (m)	RD (h)	RDD (m)	T (m <sup>2</sup> /d)	K (m/d)	Sy
11	HSA55	32	27.8	466	4.5	0.96	4	0.19	1946	0.3	0.009
12	HSA62	40	37.5	260	4.5	3.01	4	0.22	55	0.35	0.01
13	HSZ 12	81	72.8	579	2.5	7.55	2.5	5.5	63	0.09	0.078
14	HSA61	35	20.8	432	4	4.67	2.5	2.51	48	0.09	0.003

TD = Total depth of the well (m), DTW = Static water level (m), Q = Well discharge (m<sup>3</sup>/h), PD = Pumped duration (h), TDD = Total drawdown in the well (m), RD = Recovery duration (h), RDD = Residual drawdown (m), T = Transmissivity (m<sup>2</sup>/d) and Sy = Specific yield (dimensionless)

#### 5.2.4 Spatial distribution of alluvium aquifer constants

Alluvium aquifer constants include hydraulic conductivity (K), Transmissivity (T) and Specific yield (S). In the following, a brief description of these hydraulic parameters is given.

##### Hydraulic conductivity distribution map

From Table 5-4, the average hydraulic conductivity of the alluvium aquifer is determined as 1.75 m/d. Using these values, a hydraulic conductivity zonation map is constructed (Figure 5-17). From this map, the following conclusions can be made:

- The hydraulic conductivity contour line of the alluvium aquifer varies from one place to another. It ranges from 0.5 m/d along the southern periphery (Dar Salm) to 8 m/d in the north (Al-Allayfah). This result correlates with the direction of increase of aquifer thickness.
- Two closed contour line anomalies are well developed, one in the middle of the aquifer (Sana'a Plain), the second in the northern part (Al-Allayfah). The occurrence of these anomaly values is governed by the lithologic composition of the aquifer sediments as well as the structure and its thickness. The lowest values are encountered in the south of the aquifer.

##### Transmissivity distribution map

Transmissivity is the most important hydraulic parameter. It is the rate at which water of the prevailing kinematic viscosity is transmitted through a unit width of the aquifer under a unit hydraulic gradient (Todd, 1959). Several tests are used to determine the alluvium aquifer transmissivity due to its variable thickness and different potentiality. The results in Table 5-4 are used in the construction of the transmissivity distribution zonation map (Figure 5-18). The results indicate that the transmissivity values vary generally between 9 m<sup>2</sup>/d (well no. HS 36) and 3618 m<sup>2</sup>/d (well no. HSA 54), with a mean value of 511 m<sup>2</sup>/d. The relative high value of transmissivity of wells no. HSA 54 and HSA 55 may be attributed to the effect of recharge from the adjacent sewage channel, while the very low value (9 m<sup>2</sup>/d) for pumped well no. HS 36 may be attributed to the perched condition of the alluvium aquifer in this area. The spatial distribution of the transmissivity in Alluvium aquifer (Figure 5-18) shows a general trend of increase from south to north. This result revealed that the southern part of the Alluvium aquifer has a low capability to transmit water. Both K and transmissivity values are defined with regard to lithology and thickness. In general, the quantitative interpretation of the tests is affected by a number of factors such as partial penetration, aquifer geometry, heterogeneity and anisotropy (Ward, 1975 and Sen, Z. 1995).

### Specific yield distribution map

Specific yield is the volume of water released from storage from a unit area of the aquifer per unit decline of the hydraulic head. The results in Table 5-4 are used in construction of a specific yield distribution zonation map (Figure 5-19). The results indicate that the specific yield values vary generally between  $4 \times 10^{-4}$  (well no. HS 66) and 0.078 (well no. HS Z12), with a mean value of  $9.6 \times 10^{-3}$ . The relatively high values of specific yield are estimated in the southern part of the aquifer (under latitude 1690000), while the relatively low values are characteristics of the northern parts of the aquifer (Bait Al-Hilali, Bail Al-Khawi and Al-Allayfah). This may be attributed to the impact of lithofacies changes since the northern part of the aquifer receives fine sediments from flash floods from both the eastern and western wadis (As-Sir, Sa'wan and Yahis & Al-Huqqah). The increase in clay ratio characterizing this area is pronounced in the stratigraphic section of this aquifer (see chapter 3). The spatial distribution of the specific yield in the alluvium aquifer (Figure 5-19) shows a general trend of increase from south to north in the southern part of the **x x x**.

On the other hand, the relationship between the estimated transmissivities and the specific yield of the alluvium aquifer shows a weak inverse relation (Figure 5-20), while the relationship between transmissivity and well characteristics, such as total depth, shows an inverse moderate correlation (Figure 5-21).

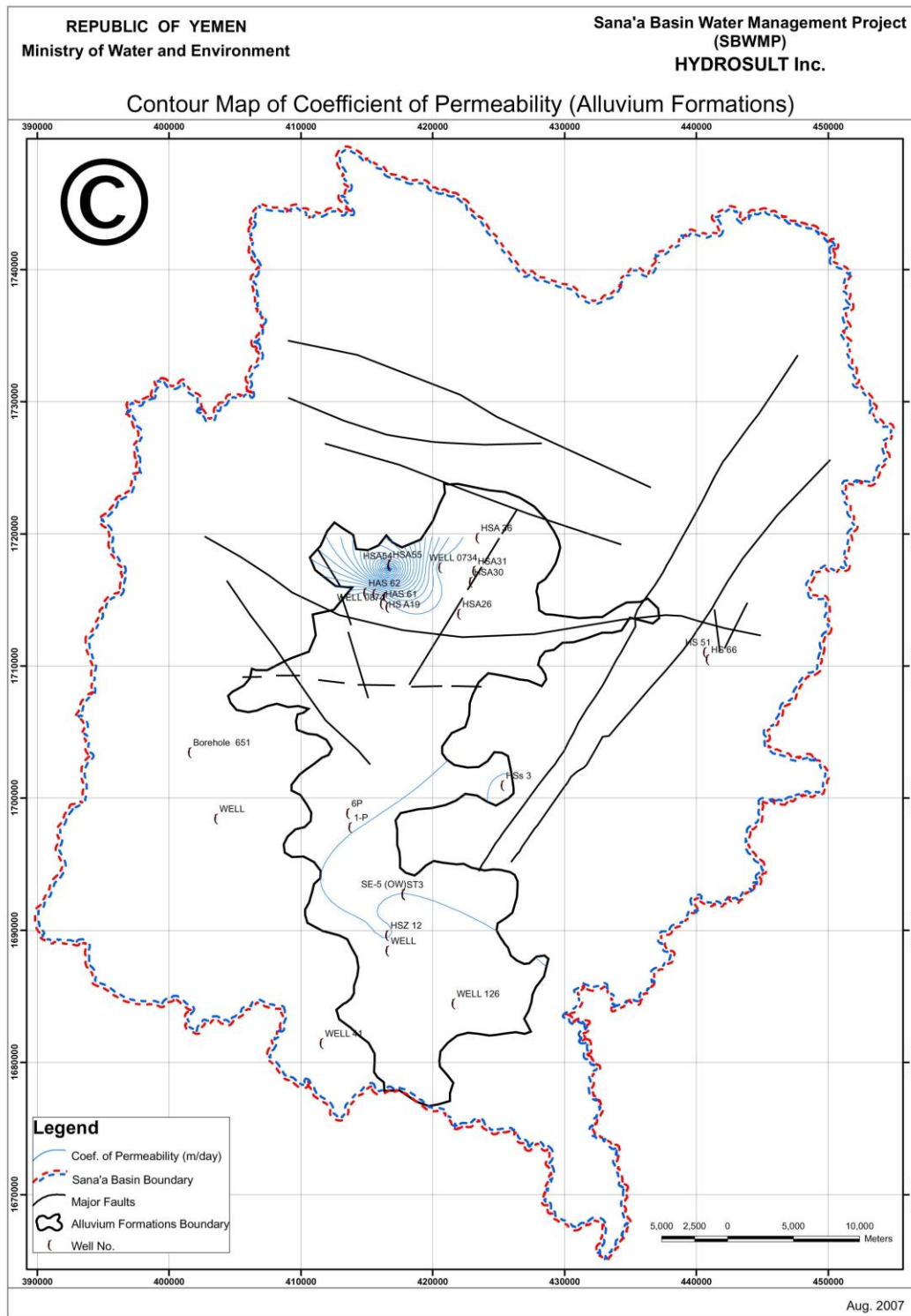


**Figure 5-18 Hydraulic conductivity distribution zonation map of the alluvium aquifer in Sana'a Basin**



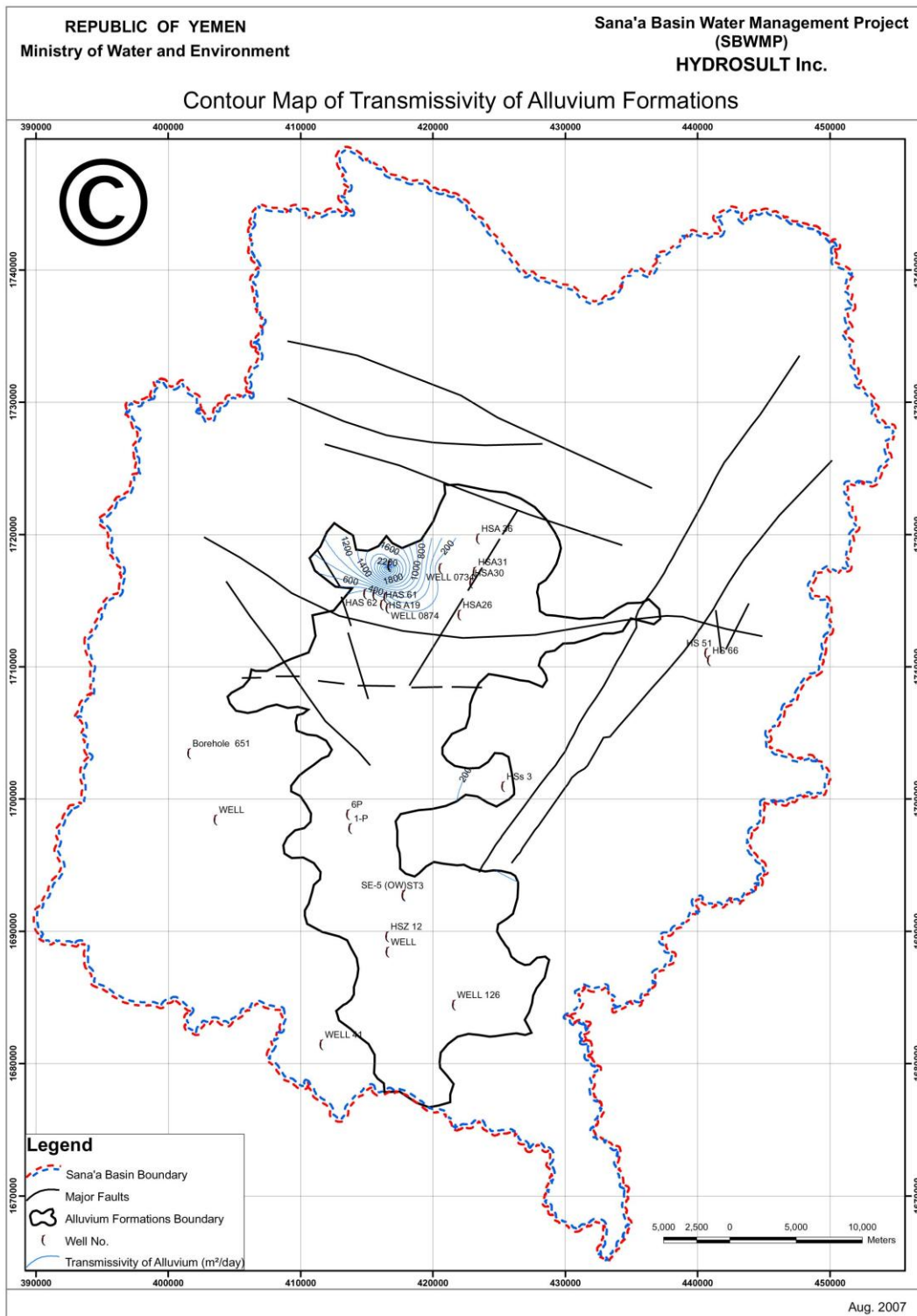


**Figure 5-19 Transmissivity distribution zonation map of the alluvium aquifer in Sana'a Basin**

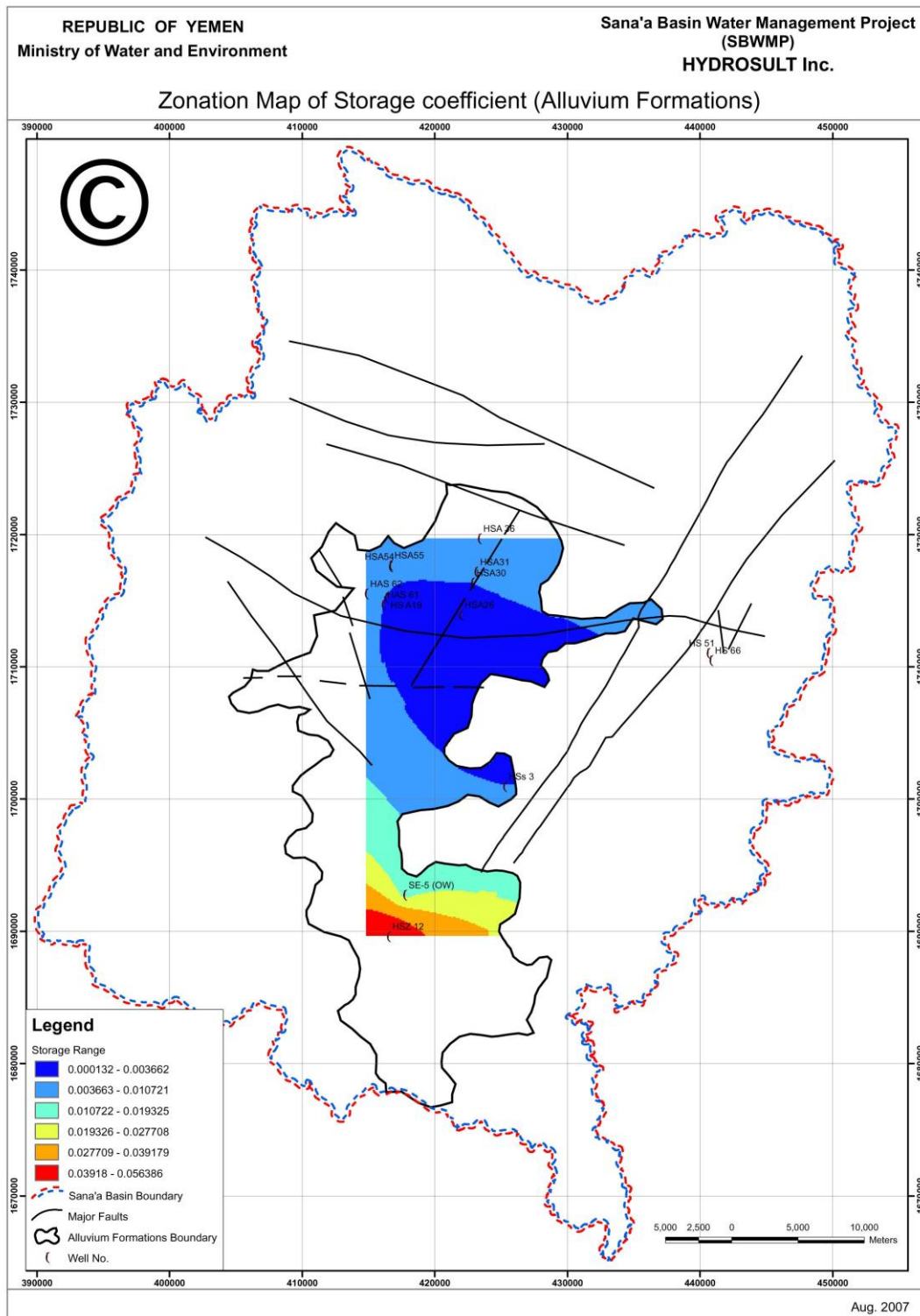


**Figure 5-20 Specific yield distribution zonation map of the alluvium aquifer in Sana'a Basin**  
Interpolated values, no values outside range of wells tested

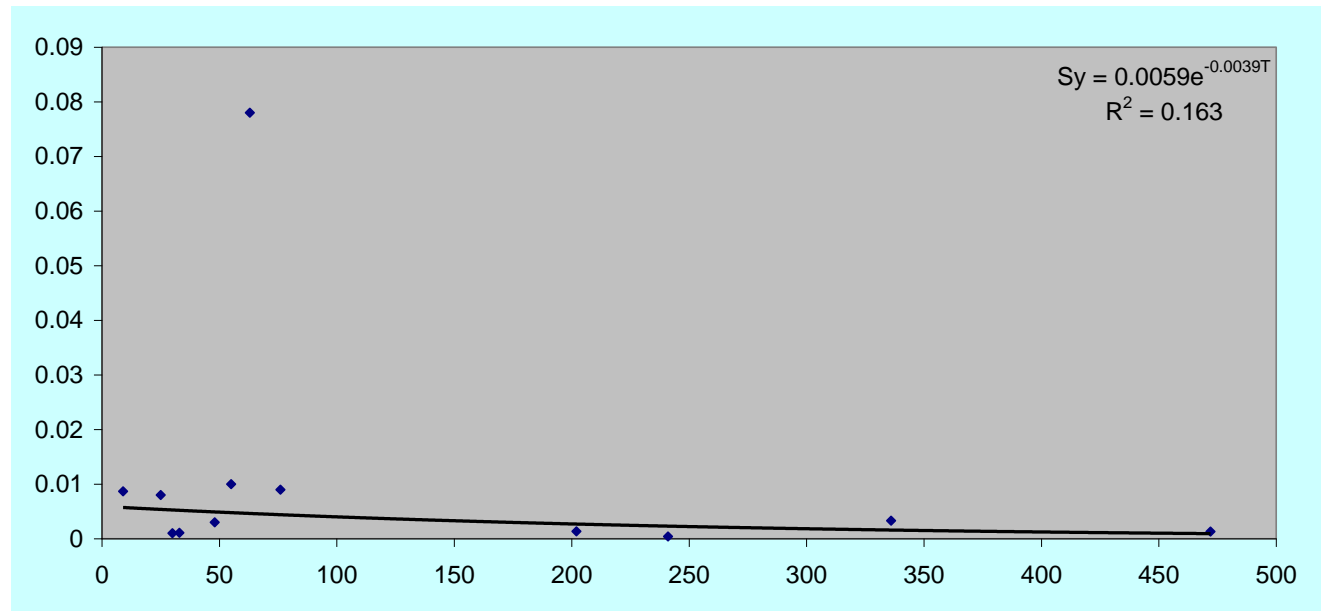


**Figure 5-21 Weak inverse relationship between transmissivity (m<sup>2</sup>/d) and specific yield (dimensionless) of the alluvium aquifer**

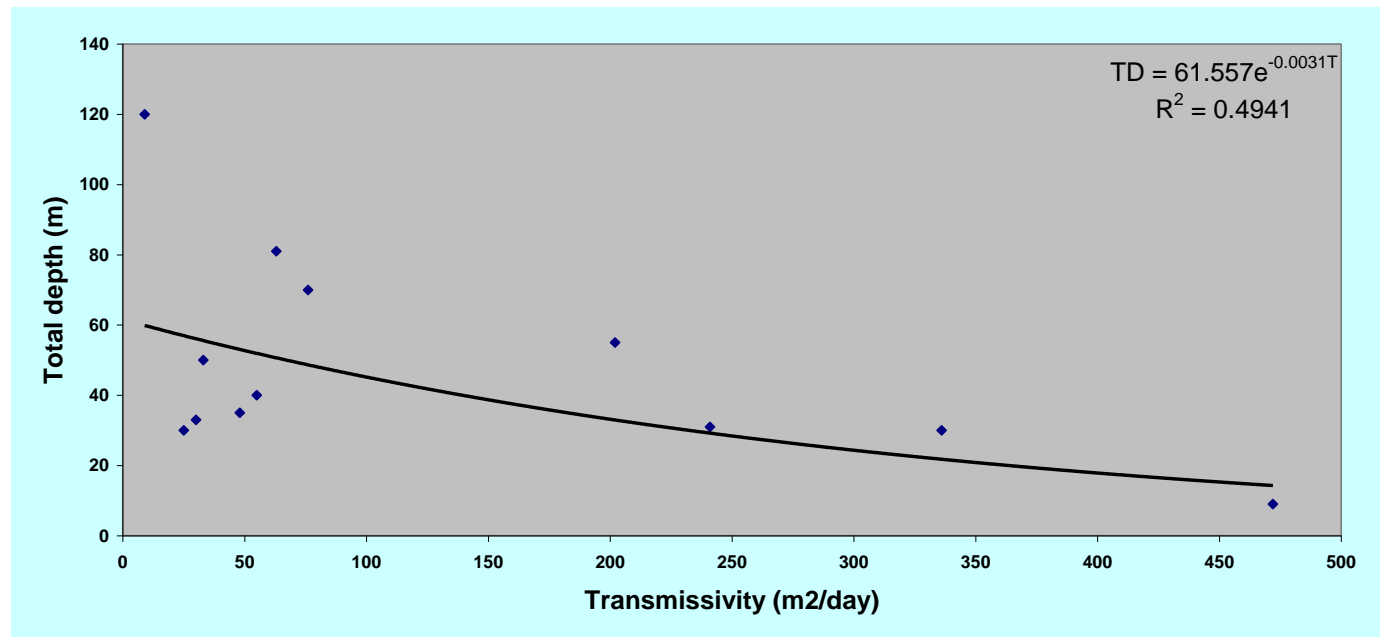


**Figure 5-22 Moderate inverse relationship between transmissivity and total depth of the pumped well in alluvium aquifer**

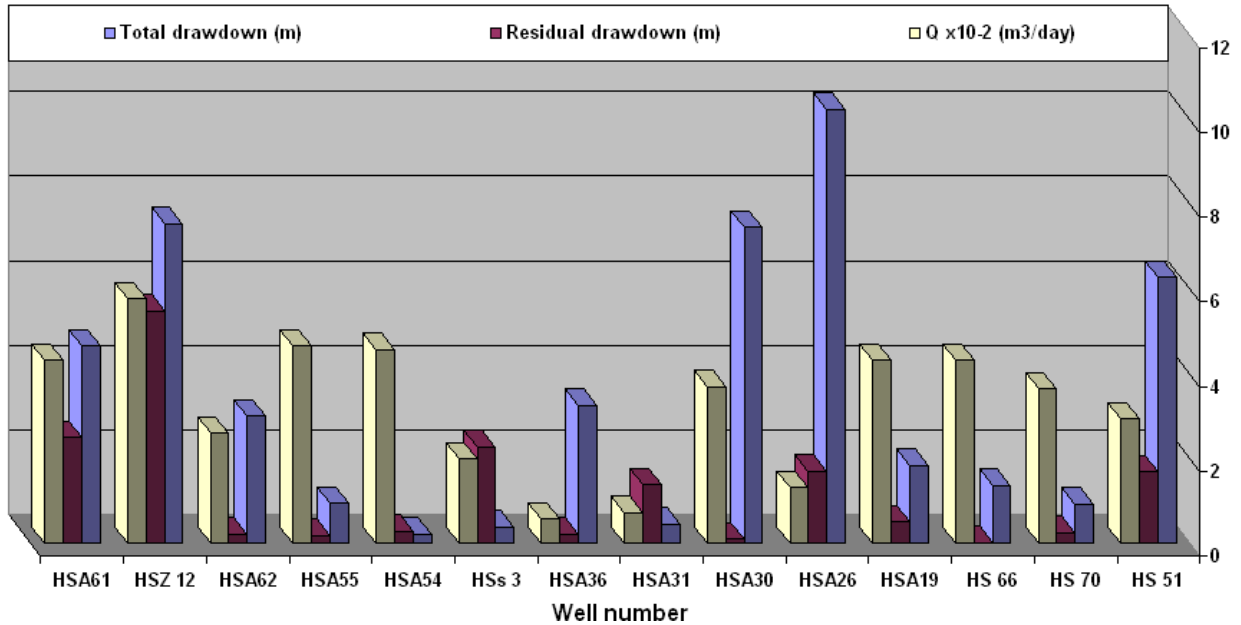


**Figure 5-23** General trend between the total drawdown (m), the residual drawdown (m) and the discharge (m<sup>3</sup>/d) from wells tested in the alluvium aquifer

However, the comparison between total drawdown, residual drawdown and discharge of the wells tested gives no definite trend (Figure 5-22). Otherwise, the relationship between the pumping duration and the total drawdown reflects a contradictory state, such as the general trend between recovery and residual drawdown (Figure 5-23 and 5-24) which confirm that **the estimated aquifer hydraulic parameters are more affected by aquifer lithology than by well hydraulics.**

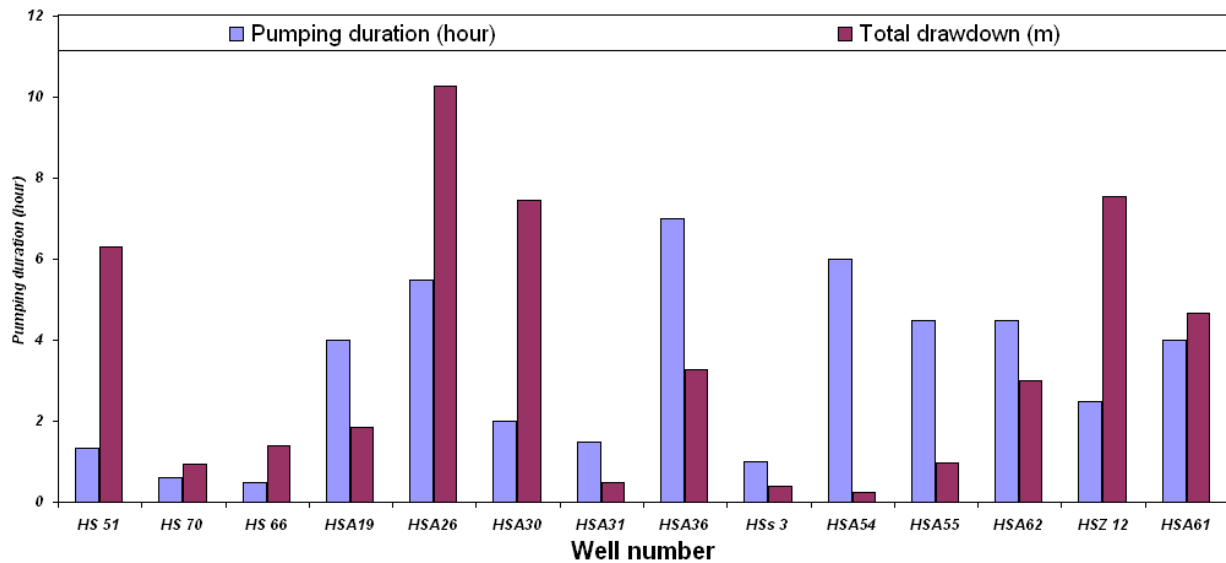


**Figure 5-24** General trend between pumping duration (h) and total drawdown (m) in wells tested in the alluvium aquifer

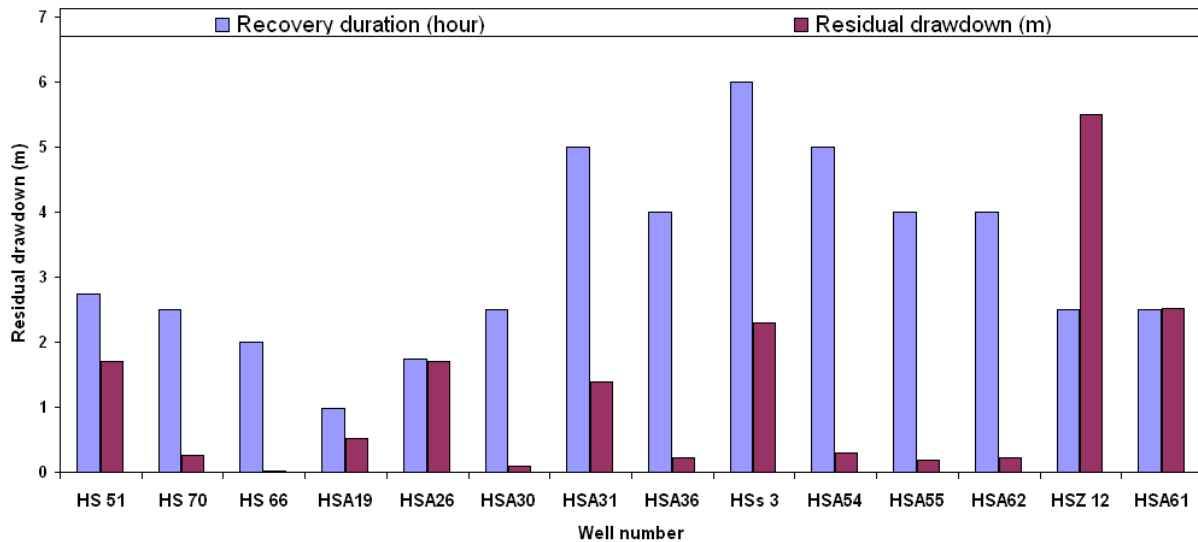


**Figure 5-25 General trend between recovery duration (h) and residual drawdown (m) in the wells tested in the alluvium aquifer**

On the other hand, the values of well loss and formation loss of the alluvium aquifer obtained by step test method are presented in Figures 5-25 & 5-26 and Tables 5-5, 5-6, 5-7. The percentages of well loss and formation loss of the total drawdown are also given in Table 5-7. It is clear that the total drawdown estimated by graphical method is close to the actual drawdown observed in the wells.

From Table 5-7, it is noticed that the average well loss equals nil since all wells tested have neither screen nor casing. Also, the laminar flow is predominant since it ranges between 82% and 98%. This again confirms that **the estimated hydraulic parameters of the aquifer are affected by aquifer lithology more than by well hydraulics.**

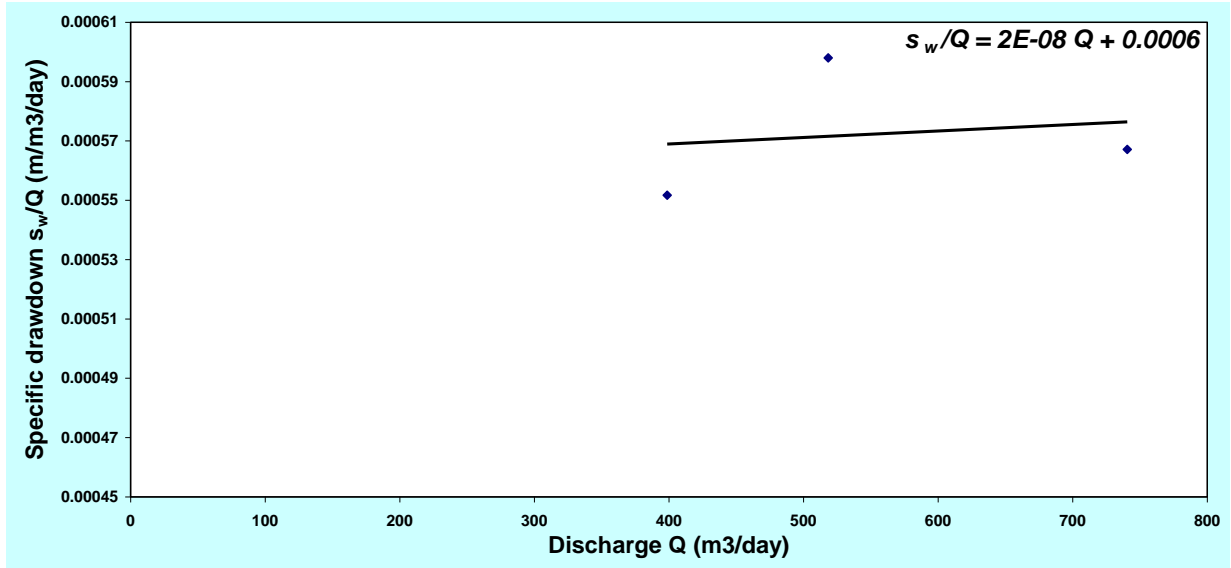


Figure 5-26 Results of step test carried out in well no. HAS 5, Bani El-Hareth

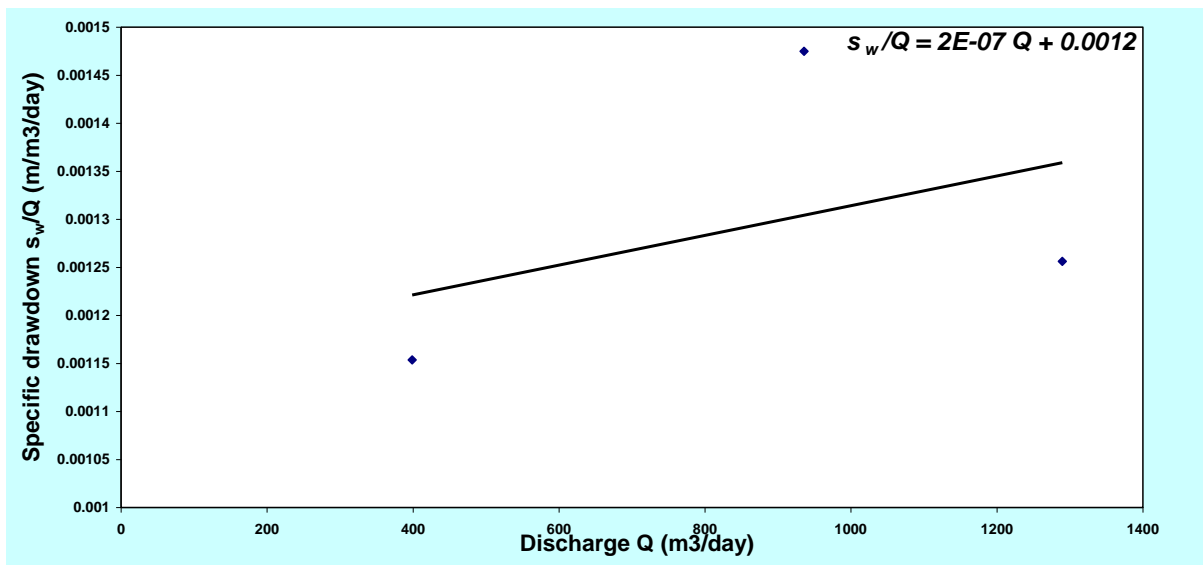


Figure 5-27 Results of step test carried out in well no. HAS 19, Bani El-Hareth

Table 5-5 Results of step drawdown test in well no. HAS 5

Step test no.	Discharge Q (m³/d)	Drawdown $s_w$ (m)	Specific drawdown $s_w/Q$ (m/m³/d)
1	398.7692308	0.22	0.000551698
2	518.4	0.31	0.000597994
3	740.5714286	0.42	5.67E-04

**Table 5-6 Results of step drawdown test in well no. HSA 19**

Step test No.	Discharge Q (m <sup>3</sup> /d)	Drawdown s <sub>w</sub> (m)	Specific drawdown s <sub>w</sub> /Q (m/m <sup>3</sup> /d)
1	398.7692308	0.46	0.001153549
2	935.7400722	1.38	0.001474769
3	1289.552239	1.62	0.00125625

**Table 5-7 Estimated values of formation loss, well loss and laminar flow ratio of the alluvium aquifer in Sana'a Basin**

	Formation loss B	C	Lp	Laminar flow Lp (%)
Well no. HSA 5	0.0006	2.00E-08	9.87E-01	9.87E+01
	0.0006	2.00E-08	9.83E-01	9.83E+01
	0.0006	2.00E-08	9.76E-01	9.76E+01
Well no. HSA 19	0.0012	2.00E-07	9.38E-01	9.38E+01
	0.0012	2.00E-07	8.65E-01	8.65E+01
	0.0012	2.00E-07	8.23E-01	8.23E+01

### 5.3 Hydraulic characteristics of the volcanic aquifer

Volcanic activities continued during the Quaternary age forming a plateau of extensive basalt cones in the northwest of the basin, interlaid with tuffs and alluvial sediments. The Quaternary basalts have a total thickness of approximately 100 m to 300 m and cover approximately 20% of the area of the basin. The Quaternary basalts are highly permeable due to fracturing and to the presence of clastic deposits between flows. Where the formation is saturated, it provides an unconfined aquifer. They overlie the Amran limestone, Cretaceous sandstone and Tertiary volcanic group. The basalt flows and stratoid sequences of Tertiary volcanic act as aquicludes, except where fractured or where primary permeability occurs in sediments between flows. The mixed basalt and rhyolite flows at the top of the sequence are highly fractured and contain perched aquifers which supply dug wells and feed high level springs. The upper layers of the volcanic are highly weathered and relatively permeable where they underlie the unconsolidated Quaternary deposits in the south of the basin. Here, they are exploited together with the unconsolidated aquifer by dug and drilled wells.

#### 5.3.1 Analysis method for small-diameter pumped wells (Cooper-Jacob method)

A method for analyzing pump test data of small-diameter wells cased to the top of an extensive artesian aquifer and screened (or open) throughout the thickness of the aquifer, neglecting the storage capacity of the well, was presented by Theis (1935). The Cooper-Jacob (1946) method is a simplification of the Theis method which is valid for greater time values and decreasing distance from the pumping well

(smaller values of  $u$ ). This method involves truncation of the infinite Taylor series that is used to estimate well function  $W(u)$ . Due to this truncation, not all early-time measured data is considered to be valid for this analysis method. The resulting equation is:

$$s = \left( \frac{2.3Q}{4\pi T} \right) \log_{10} \left( \frac{2.25Tt}{Sr^2} \right)$$

where  $s$  is the drawdown (m),  $Q$  is the well discharge rate ( $m^3/day$ ),  $t$  is the time (min),  $r$  is the radial distance (m), and  $S$  and  $T$  are the storage coefficient (dimensionless) and transmissivity ( $m^2/d$ ) respectively.

This solution is appropriate for the conditions shown in Figure 5-27.

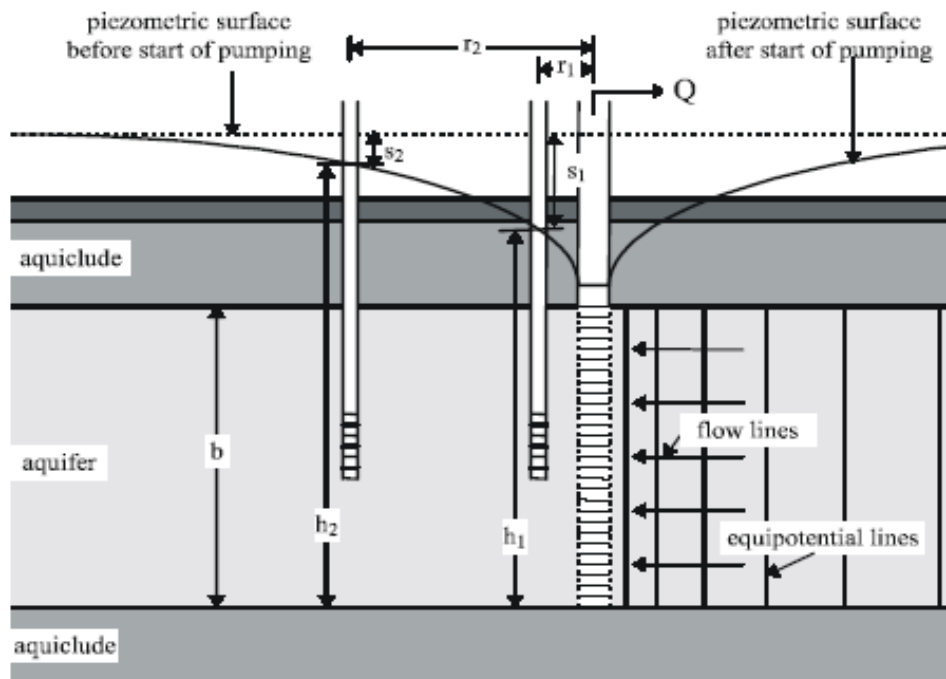


**Figure 5-28** Graph showing the conditions appropriate to solution by the Cooper-Jacob method

The Cooper-Jacob Solution assumes the following:

- The aquifer is confined and has an "apparent" infinite extent,
- The aquifer is homogeneous, isotropic, and of uniform thickness over the area influenced by pumping,
- The piezometric surface was horizontal prior to pumping,
- The well is pumped at a constant rate,
- The well is fully penetrating,
- Water removed from storage is discharged instantaneously with decline in the head,



- The well diameter is small, so well storage is negligible,
- The values of u are small (rule of thumb  $u < 0.01$ ).

### 5.3.2 Cooper-Jacob Time-Drawdown method

The above equation (Eq. 5.6) plots as a straight line on semi-logarithmic paper if the limiting condition is met. Thus, straight-line plots of drawdown versus time can occur after sufficient time has elapsed. Time is plotted along the logarithmic X axis and drawdown is plotted along the linear Y axis. Transmissivity and storativity are calculated as follows:

$$T = \frac{2.3Q}{4\pi\Delta s} \qquad S = \frac{2.25Tt_0}{r^2}$$

The data requirements for the Cooper-Jacob Time-Drawdown solution method are:

- Drawdown vs. time data at an observation well,
- Finite distance from the pumping well to the observation well,
- Pumping rate (constant).

### 5.3.3 Interpretation of the results of the new pumping tests

A step-drawdown test was carried out in well EXP-1, located in Sobaha (Bani Matar), on 16 May 2006, by the Water Resource and Development Co. under the supervision of Hydrosult Inc. and a constant discharge test was carried out on 18 May 2006. Also, a step-drawdown test was carried out in well EXP-2, located in Al-Ishash site (Bani Matar), on 22 June 2007, by the Water Resource and Development Co. under the supervision of Hydrosult Inc. and a constant discharge test was carried out on 23 May 2006.

The time-drawdown data of the new EXP-1 and EXP-2 pumping and recovery tests were analyzed using the Cooper-Jacob Time-Drawdown graphical method. The results of the long-duration pumping test and step tests are given in Figures 5-28 & 5-29 and Table 5-8 and 5-9.

**Table 5-8 Results of the long-duration pumping test carried out in the volcanic aquifer wells in Bani Matar, Sana'a Basin**

Well ID	Location	Coordinates		Altitude (m)	Total Depth (m)	Type of Pumping Test		Results	
						Step Test	Long duration	T.Drawdown (m <sup>2</sup> /d)	T.Recovery (m <sup>2</sup> /d)
EXP-1	Sobaha	1695406	403801	2569	700	3 hrs each step	72 hours	96.5	96.5
EXP-2	Al-Ishash	1692457	409230	2430	520	2 hrs each step	72 hours	101	75.9

**Table 5-9 Results of the step drawdown test in wells EX-1 and EXP-2 of the volcanic aquifer in Bani Matar, Sana'a Basin**

Well ID	Step test	Q (m <sup>3</sup> /d)	s (m)	s/Q (m/m <sup>3</sup> /d)	Efficiency
EXP-1	Step 1	959.1	0.8	7.27 x 10 <sup>-2</sup>	60%
	Step 2	1235.5	1.2	8.39 x 10 <sup>-2</sup>	53%
	Step 3	1641.6	1.8	9.47 x 10 <sup>-2</sup>	47%
EXP-2	Step 1	864	3	3 x 10 <sup>-1</sup>	66%
	Step 2	1270	5	3.4 x 10 <sup>-1</sup>	57%
	Step 3	1728	8	4 x 10 <sup>-1</sup>	50%

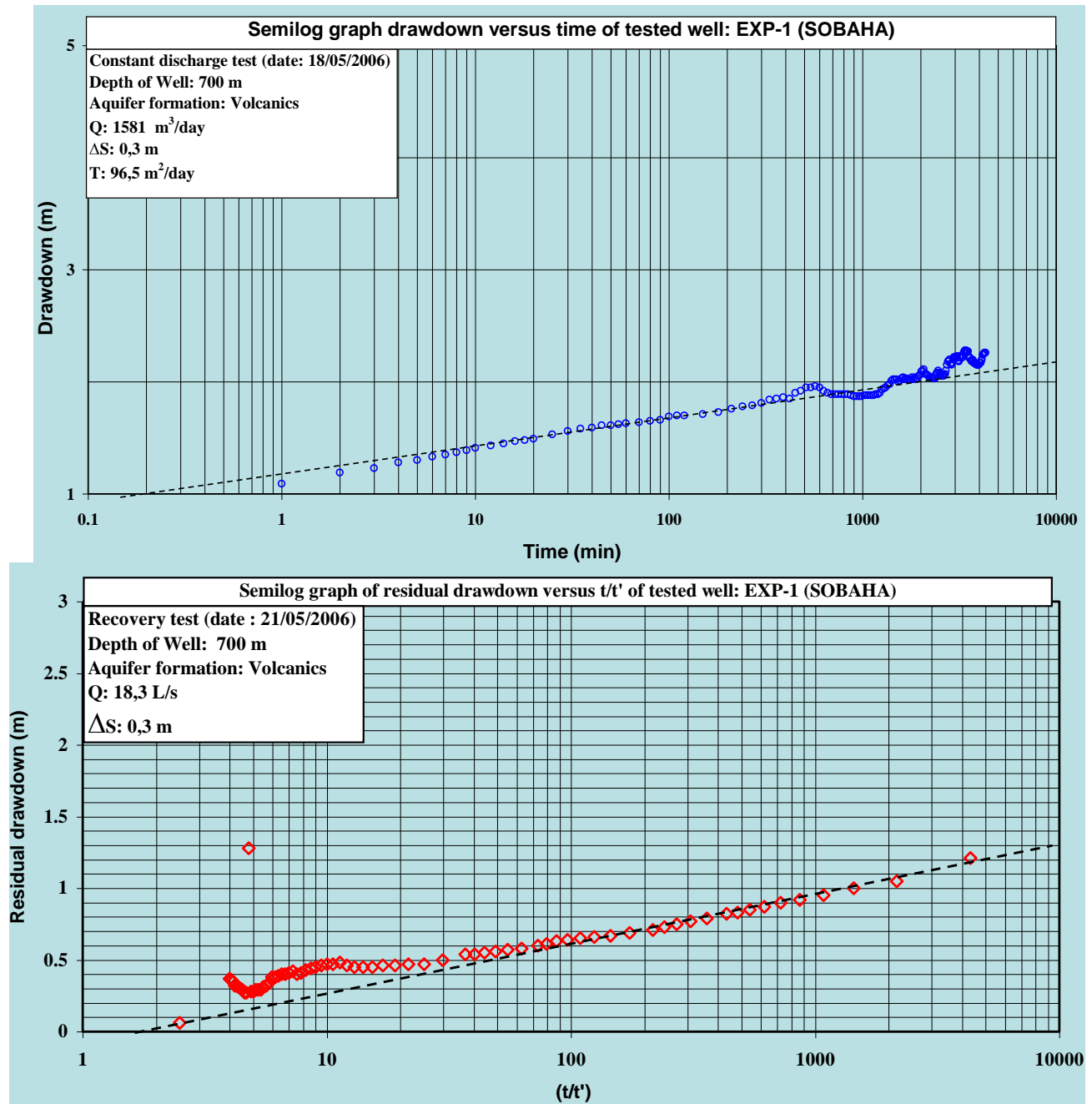


**Figure 5-29 Graphical solution of long-duration pumping and recovery test carried out on well EXP-1 in the volcanic aquifer in Sana'a Basin (May 2006)**

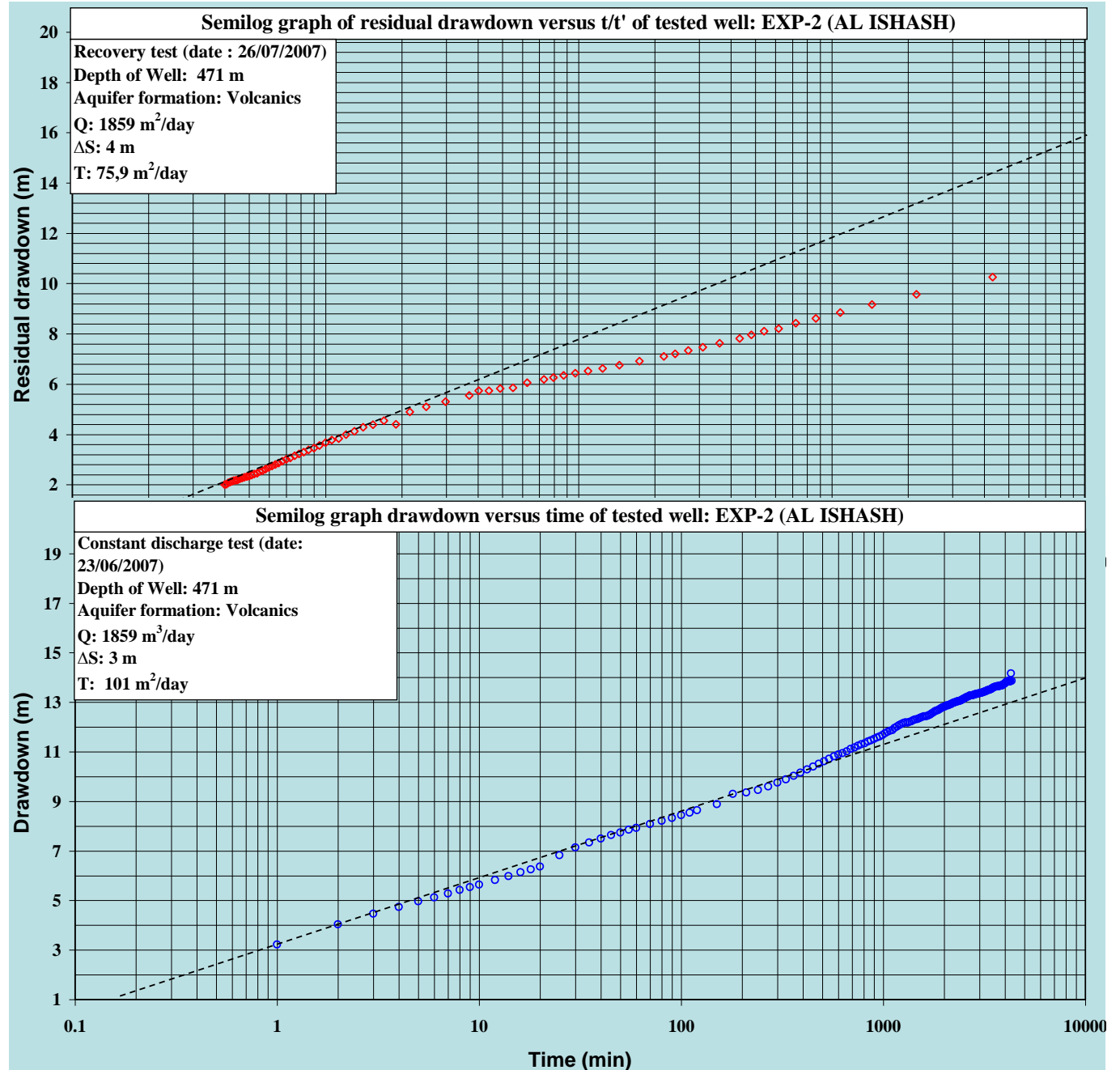


**Figure 5-30 Graphical solution of long-duration pumping and recovery test carried out on well EXP-2 in the volcanic aquifer in Sana'a Basin (June 2007)**

### 5.3.4 Interpretation of the results of the pumping tests on record

EXP-1 and EXP-2 are deep wells developed in the volcanic aquifer. The wells have water of good quality and quantity. The specific capacity of well EXP-1 is 8.09 l/s/m while it reaches 1.38 l/s/m for well EXP-2.

The results of the pumping tests performed on wells EX-1 and EX-2 and results from pumping tests on record were tabulated in Table 5-10. The tabulated transmissivity values range from 0.34 m<sup>2</sup>/d

at well 2P to 200.4 m<sup>2</sup>/d at borehole 707. The estimated hydraulic conductivity from pumping test analysis reflects a range between 0.02 m/day at borehole 5-P and 16.77 m/d at well ID O-125. On the other hand, the calculated hydraulic conductivity from transmissivity values ranges between 0.0004 m/d for well 2P to 0.4199 m/d at well ID H3R.

**Table 5-10 Results of new pumping tests and tests on record carried out in the volcanic aquifer wells in Sana'a Basin**

Well ID	Location	East	North	T (m <sup>2</sup> /d)	Thick (m)	K (m/d)	Data source	Thickness (m)	K=T/Thick
Well 20		415500	1678500	0.50	1.00	0.50	Russia 1986	905.61	0.0006
Well O125		433500	1689500	21.80	1.30	16.77	Russia 1986	590.53	0.0369
Well O128		431500	1688500	30.20	2.50	12.08	Russia 1986	643.51	0.0469
Well 47		431500	1674500	29.50	3.10	9.52	Russia 1986	817.19	0.0361
Well 261		402500	1695500	2.40	7.10	0.34	Russia 1986	678.64	0.0035
Well 25		414500	1678500	14.60	9.20	1.59	Russia 1986	908.26	0.0161
Well 160		432500	1699500	3.00	10.10	0.30	Russia 1986	452.86	0.0066
Dar Salm		418600	1688800	75.00	90.00	0.83	Russia 1986	390.74	0.1919
Borehole 707		403500	1694500	200.40	126.00	1.59	Russia 1986	710.49	0.2821
Borehole 48		415500	1681500	4.00	137.50	0.03	Russia 1986	866.58	0.0046
Borehole 1126		413500	1691500	184.50	141.10	1.31	Russia 1986	723.53	0.2550
5-p		413510	1698910	3.20	148.20	0.02	Russia 1986	231.21	0.0138
SE-4		414850	1695300	113.00	311.10	0.36	Russia 1986	534.24	0.2115
EXP-2	Bani Matar	409230	1692457	75.90			Hydrosult	569.69	0.1332
EXP-1	Bani Matar	403801	1695406	96.50			Hydrosult	689.88	0.1399
AS1	Assr.Field	411220	1696100	9.30			SAWAS 1996	378.20	0.0246
HZ	Hizyz	419766	1685107	31.60			SWSLC 2003	793.06	0.0398
H3R	W. Field	413296	1703296	89.00			SWSLC 2001	211.96	0.4199
ST-3	Sana'a Sou	417700	1692750	9.24			Italconsult 1972	445.30	0.0208
1P	USSREmbaso	413688	1697813	30.00			Russia 1986	312.16	0.0961

Well ID	Location	East	North	T (m <sup>2</sup> /d)	Thick (m)	K (m/d)	Data source	Thickness (m)	K=T/Thick
2P	Hizyaz	420603	1679475	0.34			Russia 1986	865.48	0.0004
3P	Hamdan	403700	1697944	5.06			Russia 1986	529.34	0.0096

### 5.3.5 Spatial distribution of volcanic aquifer constants

The results of pumping tests carried out combined with all available existing data were used in constructing the spatial distribution maps of hydraulic conductivity and transmissivity in the volcanic aquifer. A brief description of these two maps is given below.

#### 5.3.5.1 Hydraulic conductivity distribution map

In general, the volcanic aquifer has low regional hydraulic conductivity, while the locally higher values are found in weathered and fractured zones, as with the Tawilah sandstone aquifer. In fractured rocks, the hydraulic conductivity depends on the density and aperture of the joints. The overall hydraulic conductivity of a rock mass is determined by the permeability of the rock matrix and of the fractures. The degree of interconnection between fracture clusters is a critical feature that contributes to the hydraulic conductivity of the whole rock mass. The hydraulic conductivity of igneous and metamorphic rocks varies with depth, having a maximum value at the top and a minimum value at the bottom of the aquifer. The calculated hydraulic conductivity of the volcanic aquifer calculated from pumping test is 3.48 m/d, while the average calculated from transmissivity values reaches 0.09 m/d. The relationship between the estimated K value from volcanic aquifer transmissivity and the K values estimated from the pumping tests are shown in Figure 5-30. The figure shows no definite trend, which confirms that the previously-mentioned geological factors affect hydraulic conductivity values in the volcanic aquifer.

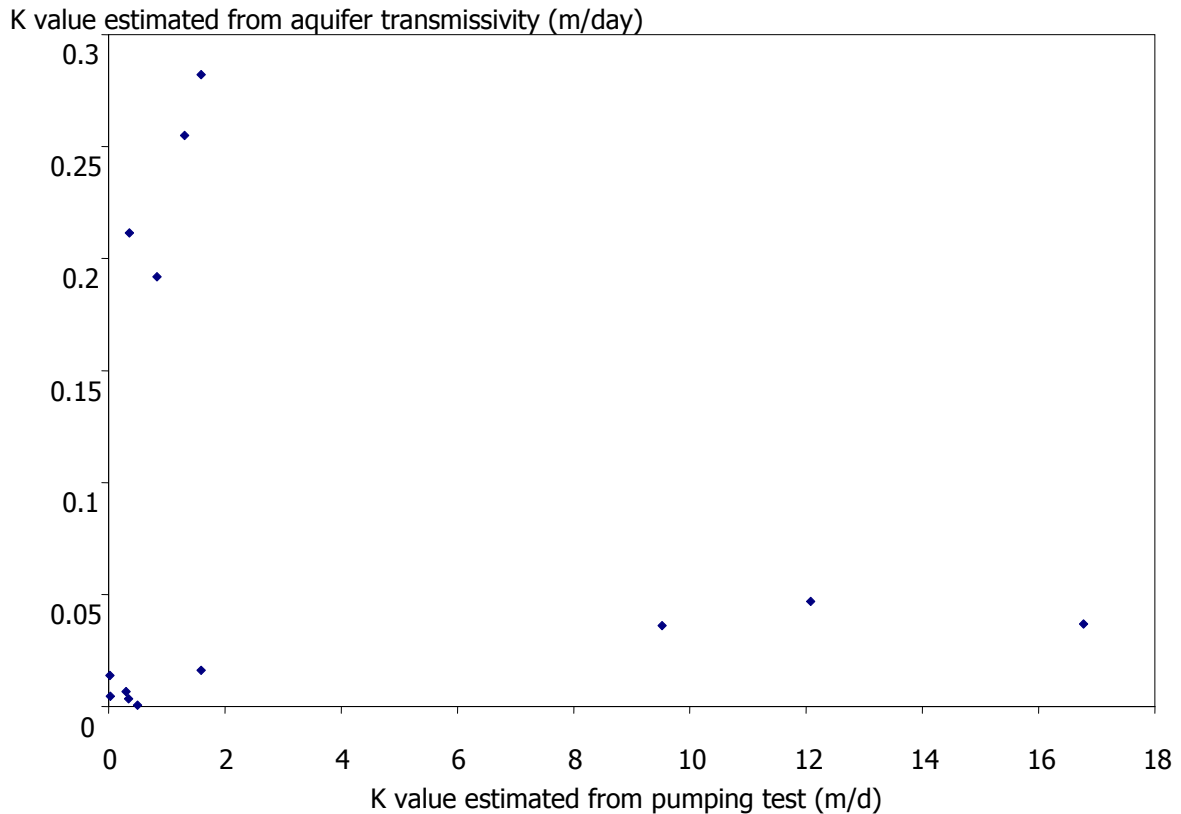


**Figure 5-31 Relationship between estimated K values from pumping tests and from transmissivity values of the volcanic aquifer in Sana'a Basin**

The hydraulic conductivity distribution map (Figure 5-31) shows that the hydraulic conductivity values of the volcanic aquifer vary from one place to another. It ranges from 0.02 m/d along the southern and eastern boundaries of the aquifer, to 0.34 m/d in the north. Generally, it increases in E-W direction and decreases in N-S direction. Two anomaly zones of K value distribution are well developed, one in the middle of the aquifer (south NW NWSA well fields) while the second in the SW of the aquifer. The occurrence of these anomaly values is governed by the lithologic composition of the aquifer sediments, as well as the degree of interconnection between fracture clusters.

In general, development of secondary porosity as a result of rock fracturing increases the hydraulic conductivity due to the number and size of the fracture apertures.

### 5.3.5.2 Transmissivity distribution map

The transmissivity distribution map of the volcanic aquifer (Figure 5-32) exhibits a great variation. This variation may be attributed to the effects of fissuring and fracturing. The general trend of increasing transmissivity is from east to west and from south to north. Three anomaly zones of T value distribution are well developed. The three anomalies are characterized by closed contour lines in the western half of the aquifer. This may be attributed to the highly fractured zones in these locations.

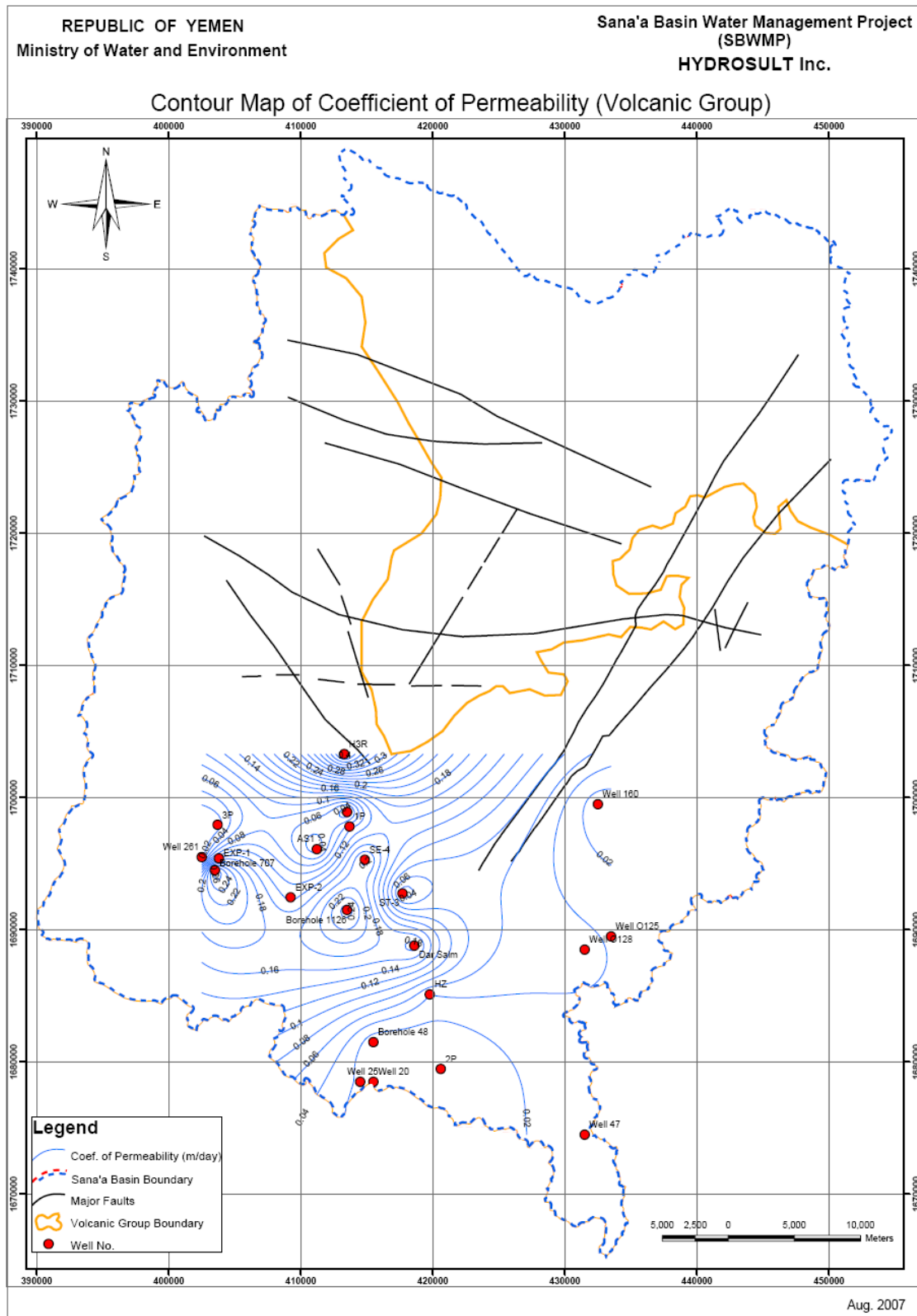


**Figure 5-32 Spatial distribution map of hydraulic conductivity of the volcanic aquifer in Sana'a Basin**



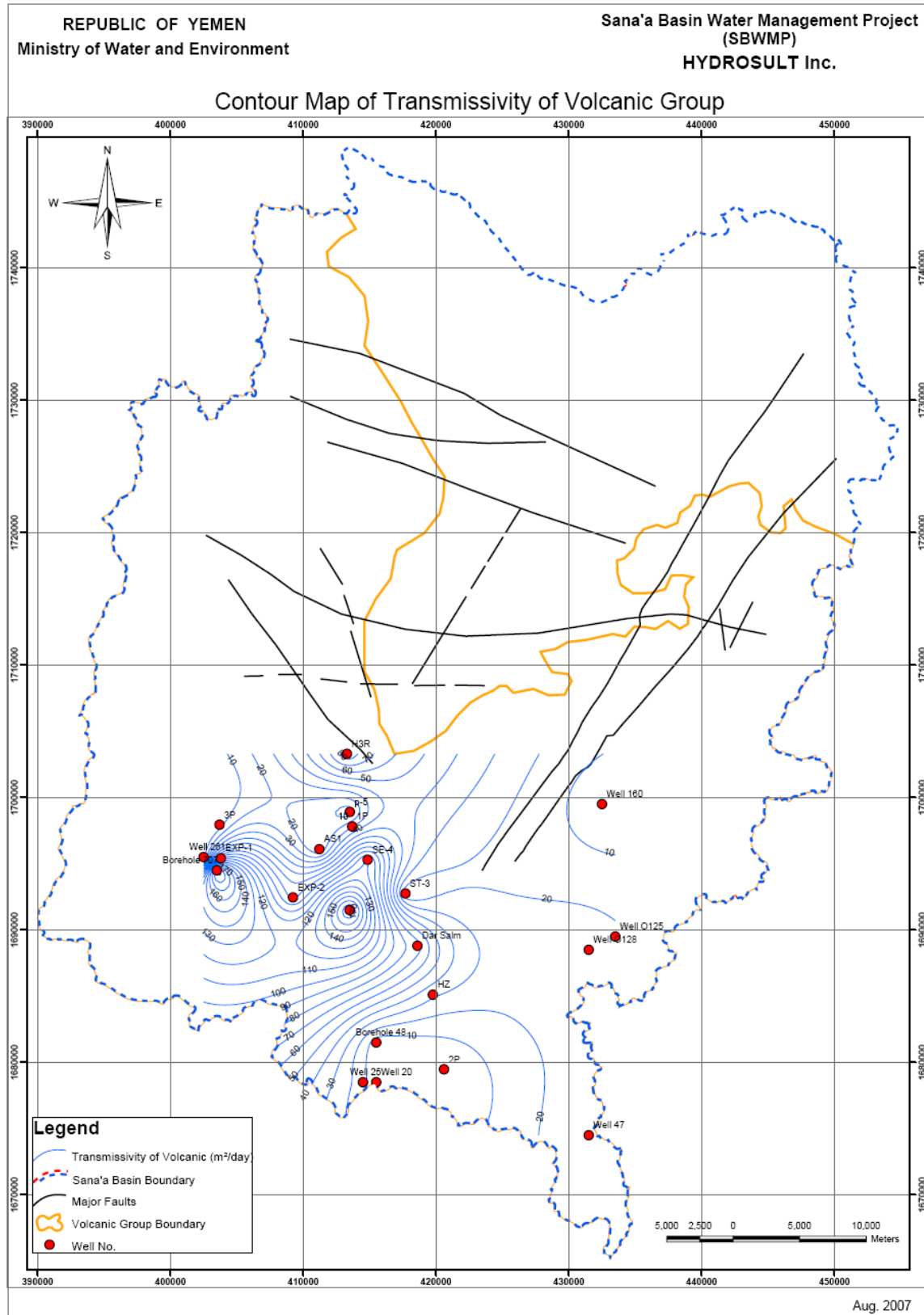


**Figure 5-33 Spatial distribution map of transmissivity of the volcanic aquifer in Sana'a Basin**

## **5.4 Hydraulic characteristics of the Tawilah sandstone aquifer**

The Tawilah sandstone aquifer is the main aquifer for drinking water in Sana'a Basin. Focusing on the hydraulic parameters of this aquifer in detail is thus of great importance. Transmissivity and storage coefficient are the basic hydraulic parameters for any aquifer capacity study. These parameters define the hydraulic characteristics of the water-bearing formation. The transmissivity indicates how much water will move through the formation, and the storage coefficient indicates how much can be extracted by pumping or draining. The analysis of pumping test data is a useful tool for estimating these two parameters. Three new pumping tests and four recovery tests were carried out in this study, as well as the re-analysis of 45 selected tests on record carried out by NWSA and Sana'a Water and Enhancement Project (SWEP). The selected 45 wells for pumping test data re-analysis are located in strategic areas in the basin, particularly around Sana'a City. The locations of the new pumped wells and the selected re-analyzed wells are shown in Figure 5-33.

For each selected well, the drawdown versus time graph was produced. Transmissivity from both constant discharge and recovery test data was re-analyzed. The graphs obtained from these data were qualitatively and quantitatively reinterpreted. Moreover, the statistical analyses carried out on data from past pumping tests was useful in depicting spatial and lateral changes in aquifer parameters, and thus allowed a better characterization of the aquifer.

### **5.4.1 Analysis method for small-diameter pumped wells (Cooper-Jacob method)**

One method of analyzing pump test data of small-diameter wells cased to the top of an extensive artesian aquifer and screened (or open) throughout the thickness of the aquifer, neglecting the storage capacity of the well, was presented by Theis (1935). The Cooper-Jacob (1946) method is a simplification of the Theis method, valid for greater time values and decreasing distance from the pumping well (smaller values of  $u$ ).

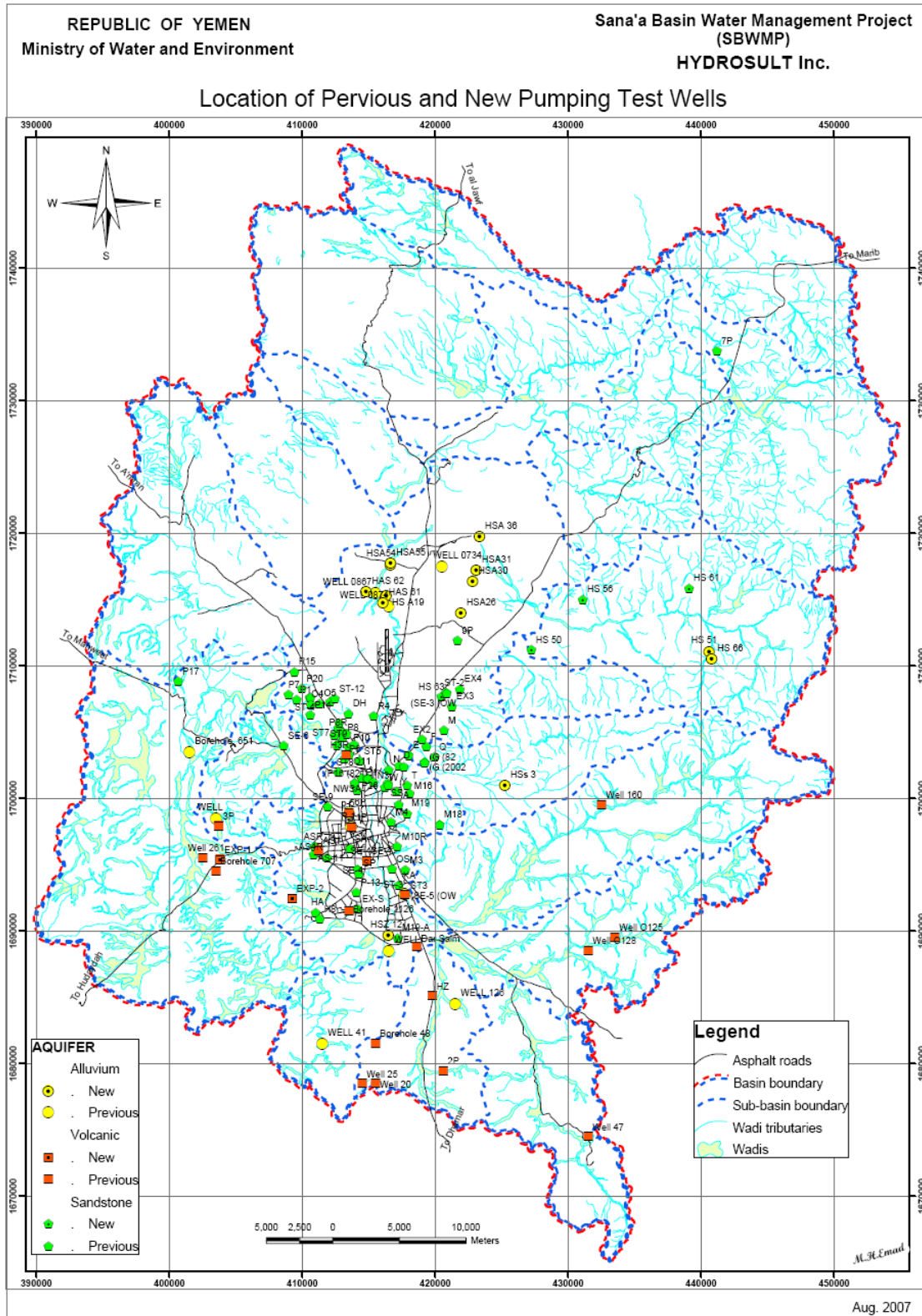


**Figure 5-34 Location map of newly pumped wells and re-analyzed wells**

### 5.4.2 Interpretation of results of the new pumping tests

The time-drawdown data of the three new pumping tests and four new recovery tests were analyzed using Cooper-Jacob Time-Drawdown graphical solution method. The results are given in Figures 5-34 to 5-37 and Table 5-11.

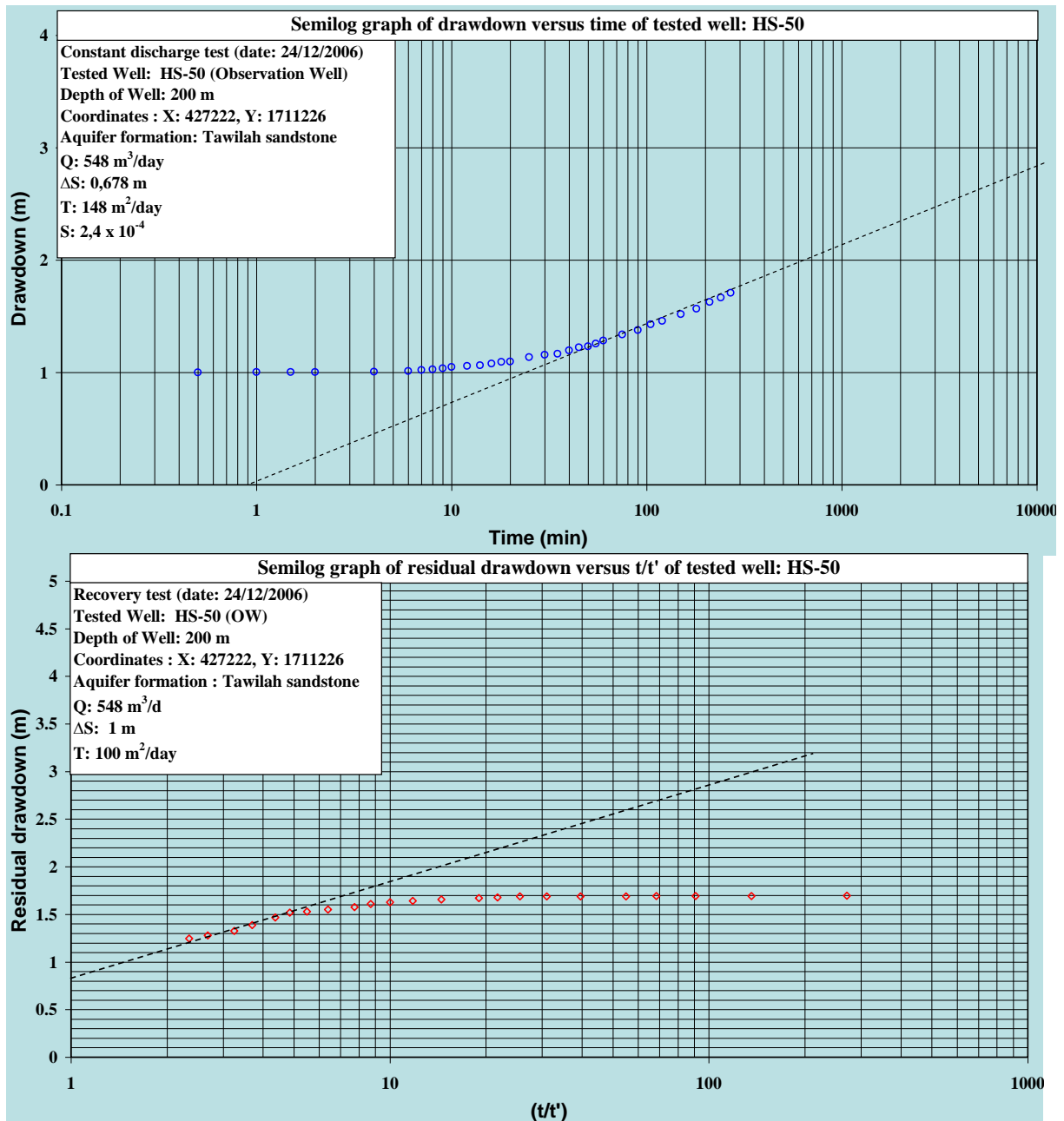


**Figure 5-35 Graphical solution of pumping and recovery test carried out on well HS-50 in Tawilah sandstone aquifer in Sana'a Basin (Dec. 2006)**

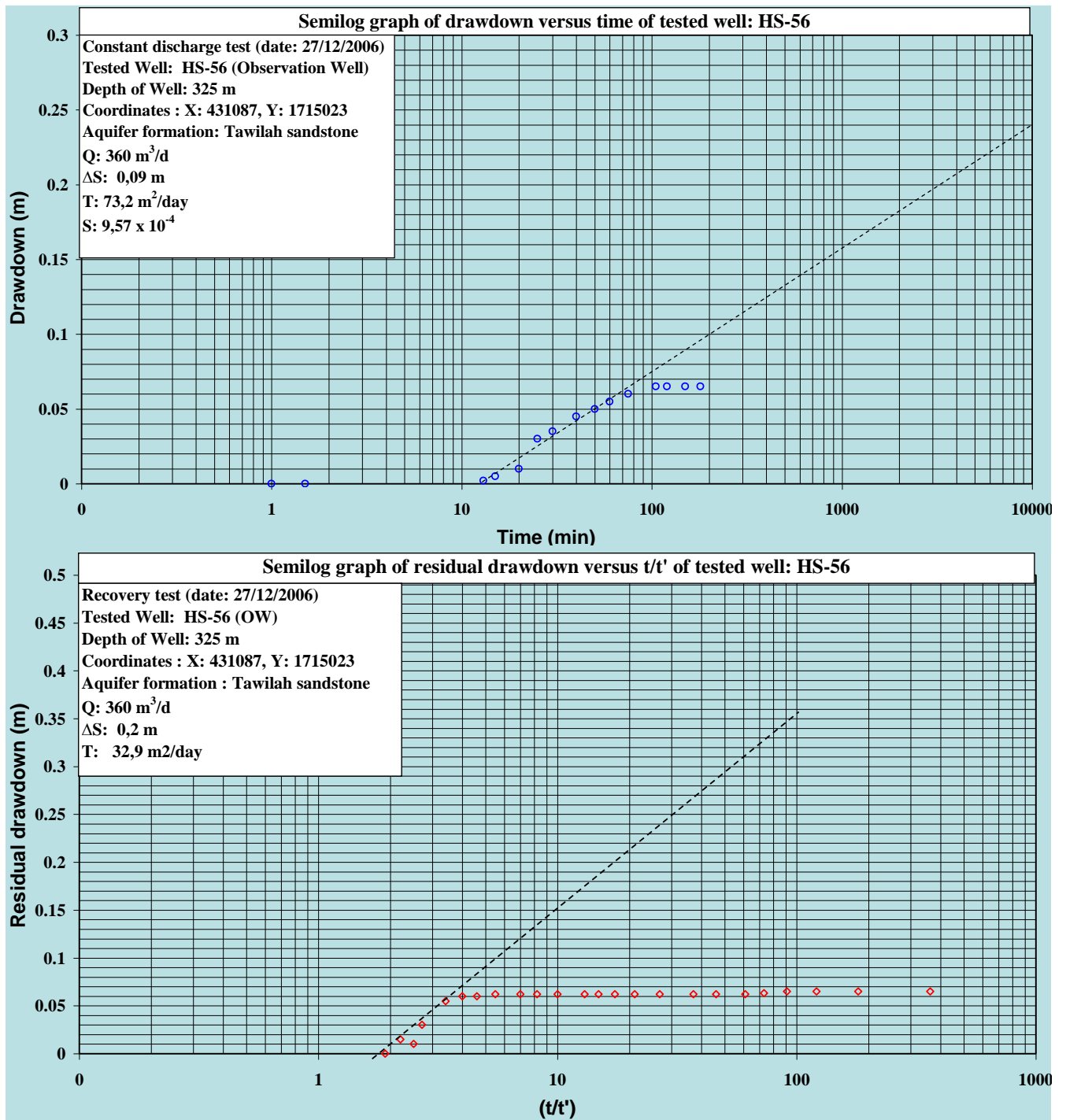


**Figure 5-36 Graphical solution of pumping and recovery test carried out on well HS-56 in Tawilah sandstone aquifer in Sana'a Basin (Dec. 2006)**

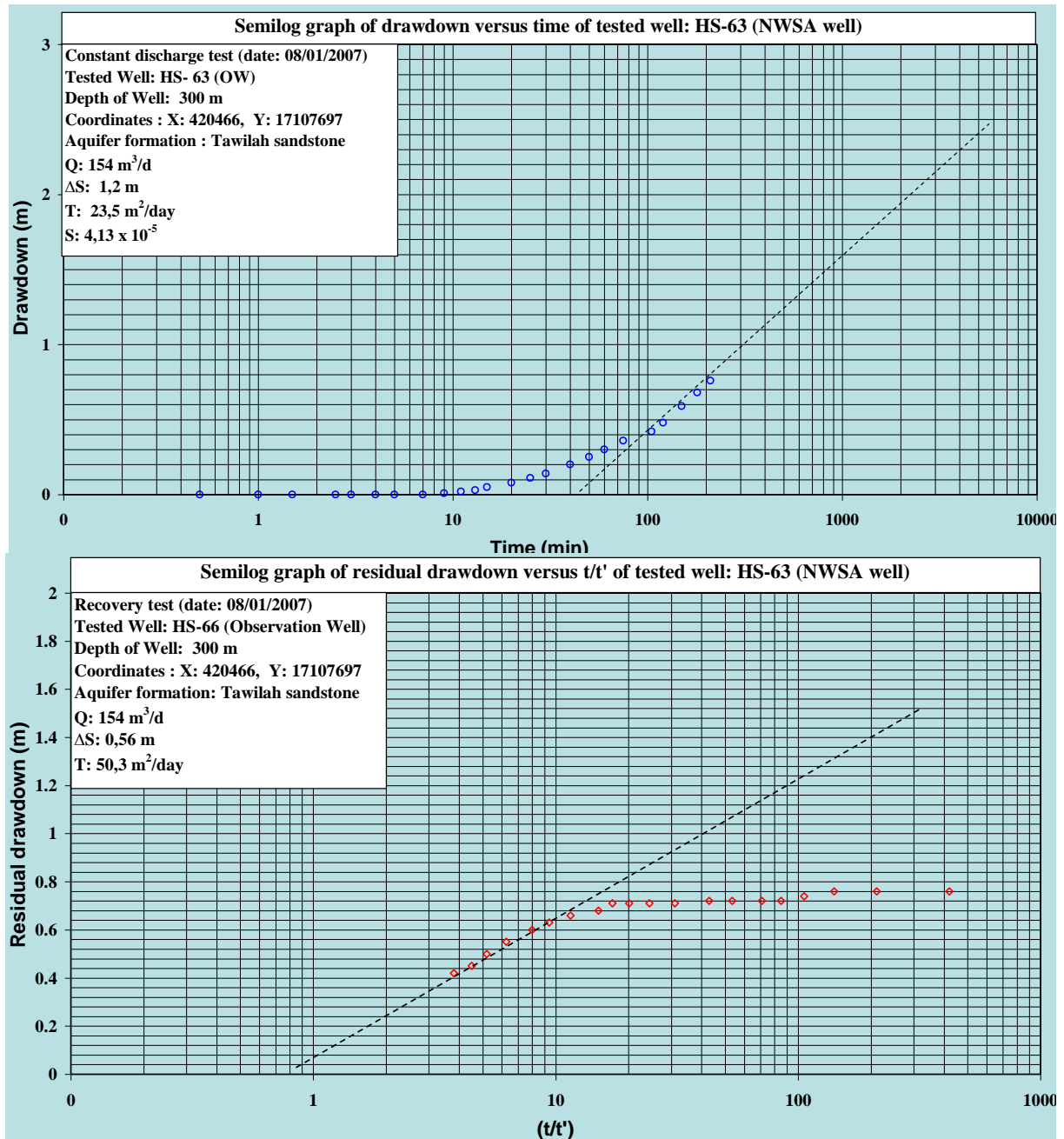


**Figure 5-37 Graphical solution of pumping and recovery test carried out on well HS-63 in Tawilah sandstone aquifer in Sana'a Basin (Jan. 2007)**

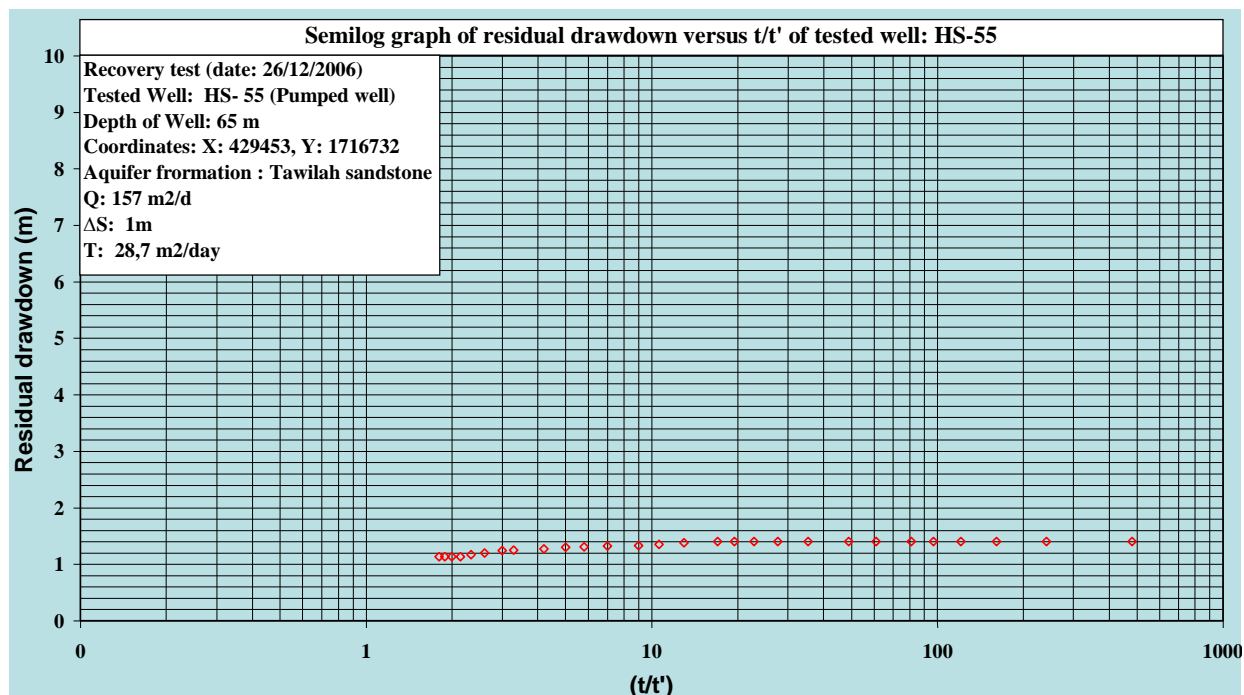


**Figure 5-38 Graphical solution of recovery test carried out on well HS-55 in Tawilah sandstone aquifer in Sana'a Basin (Dec 2006)**

**Table 5-11 Results of new pumping and recovery tests carried out in deep wells of Tawilah sandstone aquifer applying the Cooper-Jacob method (Dec.2006)**

Well ID	X (UTM)	Y (UTM)	Q (m <sup>3</sup> /d)	TD (m)	Δs (m)	T/drawdown (m <sup>2</sup> /day)	T/recovery (m <sup>2</sup> /d)	S (dimensionless)
HS-50	427222	1711226	548	200	0.68	148	100	2.4x10 <sup>-4</sup>
	431087	1715023	360	325	0.09	73.2	32.9	9.57x10 <sup>-4</sup>
HS-66	420466	17107697	154	300	1.2	23.5	50.3	4.13x10 <sup>-5</sup>
HS-55	429453	1716732	157		1	---	28.7	---

Results of the newly conducted pumping tests in the lower zone of the Tawilah sandstone aquifer (Table 5-11), it is noted that the estimated transmissivity values from the pumping tests range between 23.5 and 148 m<sup>2</sup>/d, while the estimated ones from the recovery tests range between 32.9 and 100 m<sup>2</sup>/d. These findings indicate that the Tawilah sandstone aquifer is highly anisotropic.

On the other hand, the estimated storage coefficient for the lower zone of the Tawilah sandstone aquifer from vary between 4.13 x 10<sup>-5</sup> and 9.57x 10<sup>-4</sup> which shows that the Tawilah sandstone aquifer is under confined conditions.

### 5.4.3 Interpretation of results of re-analyzed pumping tests

Among 91 pumping tests carried out by different sources, the data from 45 pumping tests were chosen for re-analysis. For all selected pumping tests on record, interpretation of data was done by applying the Cooper-Jacob Method. Re-analysis of the selected pumping tests is also done by the same method, using a Microsoft Excel template to achieve the comparison. The re-analysis was conducted to

determine the hydrodynamic characteristics of the pumped well system and the feeding aquifer. For the majority of these chosen wells, the long-duration at constant discharge test, followed by the recovery test data and the step-drawdown test data were the source of the re-analysis process. The transmissivity and storage coefficient of the Tawilah sandstone aquifer were estimated from the re-analysis of these data. The aquifer hydrodynamic characteristics were obtained from the time-drawdown relationship, which can verify any recharge or boundary effects. The recovery tests confirm the results obtained by the constant discharge test and indicate whether the aquifer is extensive or not. The re-analysis of the selected 45 wells revealed the presence of errors in the previous analyses. Table 5-12 summarizes these errors. These errors necessitated re-evaluation of the hydraulic parameters based on the 45 pumping tests in the selected wells.

**Table 5-12 Errors committed on previous interpretation of pumping tests on record**

Well ID	Source of data	Location	X (UTM)	Y (UTM)	Reasons to re-evaluate pumping test data
O.S.	(SWSSP-7/2001)*	S. Sana'a	416750	1694655	Line correlation used to determine $\Delta s$ in drawdown curve Line correlation used to determine $\Delta s$ in recovery curve
R-4	(SWEP-D/2001-17)	Rawd Field	415355	1706200	Line correlation used to determine $\Delta s$ in drawdown curve Line correlation used to determine $\Delta s$ in recovery curve
P-16	(SWEP-C/2001-16 /2003)	W. Field	413945	1701124	Line correlation used to determine $\Delta s$ in drawdown curve Line correlation used to determine $\Delta s$ in recovery curve One slope used in drawdown curve (2 in reality)
M-19	(SWEP-A/2001-14, 2002)	Mus. Field	417875	1698860	Line correlation used to determine $\Delta s$ in drawdown curve Line correlation used to determine $\Delta s$ in recovery curve
M-4	(SWEP-B/2001-15)	Mus. Field	416665	1698207	Line correlation used to determine $\Delta s$ in drawdown curve Line correlation used to determine $\Delta s$ in recovery curve
NWSA	(SWSSP-7/2001)	Hasabah	414480	1701500	Line correlation used to determine $\Delta s$ in drawdown curve Line correlation used to determine $\Delta s$ in recovery curve
EX-S	(SWSSP-7/2000)	Haddah	414157	1691674	Line correlation used to determine $\Delta s$ in drawdown curve Line correlation used to determine $\Delta s$ in recovery curve One slope used in drawdown curve (2 in reality) and one slope used in recovery curve (2 in reality)



Well ID	Source of data	Location	X (UTM)	Y (UTM)	Reasons to re-evaluate pumping test data
H-8	(SWSSP-7/2000)	Haddah	411300	1690090	Line correlation used to determine $\Delta s$ in drawdown curve Line correlation used to determine $\Delta s$ in recovery curve One slope used in drawdown curve (2 in reality) and one slope used in recovery curve (2 in reality)
ASR-12	(SWSSP-7/2002)	Assr. Field	410938	1696367	Line correlation used to determine $\Delta s$ in drawdown curve Line correlation used to determine $\Delta s$ in recovery curve
SA-1	(SWSSP-7/2001)	Zubairy Park	413594	1696222	Line correlation used to determine $\Delta s$ in drawdown curve Line correlation used to determine $\Delta s$ in recovery curve
AS-11	(SWEP-D/2001-17)	Assr. Field	410854	1695750	Line correlation used to determine $\Delta s$ in drawdown curve Line correlation used to determine $\Delta s$ in recovery curve
AS4-R	(Contract No. 3/2003)(SWSLC)	Assr. Field	411868	1695561	Line correlation used to determine $\Delta s$ in drawdown curve Line correlation used to determine $\Delta s$ in recovery curve
Y	(SWEP-D/2001-17)	E. Field	417084	1700542	Line correlation used to determine $\Delta s$ in drawdown curve Line correlation used to determine $\Delta s$ in recovery curve
N-3	SWEP-A/2001-14	Mus. Field	416455	1700970	Using 2 lines in recovery curve and 2 $\Delta s$ Using no aligned points to make the Jacob's line in drawdown curve
M10-R	(Contract No. 3/2001) (SWSLC)	Mus. Field	44 13 41	15 20 34	Using no aligned points to make the Jacob's line in recovery curve
TP-1	(SWSSP-7/2000)	Hasabah	415350	1701200	Line correlation used to determine $\Delta s$ in drawdown curve Line correlation used to determine $\Delta s$ in recovery curve
P8-R	(SWEP-D/2001-17)	W. Field	413000	1705000	Line correlation used to determine $\Delta s$ in drawdown curve Line correlation used to determine $\Delta s$ in recovery curve One slope used in drawdown curve (2 in reality)

Well ID	Source of data	Location	X (UTM)	Y (UTM)	Reasons to re-evaluate pumping test data
KA	(SWSSP-7/2001)	Kadsia	417245	1693470	Line correlation used to determine $\Delta s$ in drawdown curve Line correlation used to determine $\Delta s$ in recovery curve
DH	(SWSSP-7/2001)	W. Field	413470	1706400	Line correlation used to determine $\Delta s$ in drawdown curve Line correlation used to determine $\Delta s$ in recovery curve
M19-A	(SWSSP-7/2002)	Asbahi	417176	1689477	Using only step drawdown test Using 1 <sup>st</sup> step to determine transmissivity No constant discharge test
D	(SWEP-C/2001-16)	E. Field	417264	1702475	Using unaligned points to determine the Jacob's line in drawdown and recovery curves
B70-1	(SAWAS, 1992)	Sabaeen	4141500	1694650	Using 2 lines in drawdown curve and 2 $\Delta s$ Using few point to make the line of recovery
G (2002)	SWEP-C/2001-16 (2002)	E. Field	419194	1702725	Using 2 lines in drawdown curve and 2 $\Delta s$ Using few points to make the Jacob's line of recovery
HA	(SWSSP-7/2002)	Haddah	411005	1691410	Line correlation used to determine $\Delta s$ in drawdown curve Line correlation used to determine $\Delta s$ in recovery curve One slope used in drawdown curve (2 in reality)
AS-R	(SWSSP-7/2002)	Assr. Field	410938	1696367	Line correlation used to determine $\Delta s$ in drawdown curve Line correlation used to determine $\Delta s$ in recovery curve
M-3	(Contract No. 3/2001) (SWSLC)	Mus. Field	417753	1694599	Line correlation used to determine $\Delta s$ in drawdown curve Line correlation used to determine $\Delta s$ in recovery curve

Well ID	Source of data	Location	X (UTM)	Y (UTM)	Reasons to re-evaluate pumping test data
SP	(SWSSP-7/2002)	Sabaeen Park	414245	1694334	Line correlation used to determine $\Delta s$ in drawdown curve Line correlation used to determine $\Delta s$ in recovery curve One slope used in drawdown curve (2 in reality)
P-17	(SWEP-B/2001-15)	W. Field	400656	1708837	Line correlation used to determine $\Delta s$ in drawdown curve Line correlation used to determine $\Delta s$ in recovery curve
P-14	(H&H, 1982)	NW Dahban	410594	1706303	Validation of results Conform results
P-15	(H&H, 1982)	Wadi Dahr	409405	1709557	Validation of results Conform results
P-6	(H&H, 1982)	Wadi AL Jabara	413177	1702960	Validation of results Conform results
EX-3	(H&H, 1982)	Ssarf	421251	1706952	Validation of results Conform results
P-10	(H&H, 1982)	TV station	413503	1703816	Validation of results Conform results
G-82	(H&H, 1982)	Wadi Sawan	419194	1702725	Validation of results Conform results
AS-1	(SWEP-B/2001-15)	Asser Field	411220	1696100	Line correlation used to determine $\Delta s$ in drawdown curve Line correlation used to determine $\Delta s$ in recovery curve
HZ	(SWSLC) (2003)	Hizyaz	4191766	1685107	One slope used in drawdown curve (2 in reality)
T	(H&H, 1982)	E. Field	417885	1701005	No big difference between the 2 results
SS	(H&H, 1982)	E. Field	416413,44	1701152	No good Jacob's line used in recovery curve
M-18	(H&H, 1982)	Mus. Field	420320	1698030	Line correlation used to determine $\Delta s$ in drawdown curve Line correlation used to determine $\Delta s$ in recovery curve

Well ID	Source of data	Location	X (UTM)	Y (UTM)	Reasons to re-evaluate pumping test data
W	(H&H, 1982)	E. Field	416205	1700850	Using unaligned points to determine the Jacob's line
P-26	(SWEP-D/2001-17)	W. Field	414109	1700607	Line correlation used to determine $\Delta s$ in drawdown curve Line correlation used to determine $\Delta s$ in recovery curve
M-16	(Contract No. 3/2001) (SWSLC)	Mus. Field	4414 12	1702243	No big difference between results For recovery test, we use the correct point to trace Jacob's line
E	(H&H, 1982)	Wadi Sawan	418005	1703262	Validation of results Conform results Validation of results
H3-R	(Contract No. 3/2001) (SWSLC)	Haddah	441158	1701841	No good point used in drawdown curve to determine Jacob's line
P-13	(SWEP-B/2001-15)	W. Field	413296	1703296	Line correlation used to determine $\cdot s$ in drawdown curve Line correlation used to determine $\cdot s$ in recovery curve

\*: Contract number or Consultant

SWSLC: Sana'a Water and Sanitation Local Corporation

SAWAS: Sources for Sana'a Water Supply

SWEP: Sana'a Water and Enhancement Project

SWSSP: Sana'a Water Supply and Sanitation Project

H&H: Howard Humphreys and Sons Consulting Engineers, 1982

The description of the form of curves obtained for each re-analysed pumping test data set helps to know the feeding condition of Tawilah sandstone aquifer. It is noted that, for almost all pumping tests carried out in the Tawilah sandstone aquifer, the recharge effect exists. That means there is a feeding of the aquifer from a long distance. Leakage from the upper layers of volcanic and alluvium aquifers is very slow to feed the sandstone aquifer. Leakage between the sandstone aquifer and upper layers is important in the long term, but not during the pumping tests. The description for each curve obtained for each re-analysed pumping test data set is tabulated in Table 5-13.

**Table 5-13 Description of graphs obtained from re-analysis of past pumping test data from Tawilah sandstone deep wells in Sana'a Basin**

Well ID	Time of starting of steady state (min)	Drawdown at steady state (m)	Remarks
M-4	2,940	15.48	Recharge effect
P-13	Boundary effect at 1,000 min		2 different slopes in drawdown and recovery curves
W	2,400	2.3	Recharge effect
M-16	2,040	8.43	Recharge effect
M-18	3,960	10.28	Recharge effect
P-26	1,800	9.1	Recharge effect
SS	18	1.06	Low variation of water levels Recharge effect
T	1,600	3.97	Recharge effect Almost-stability of water levels
G	Boundary effect at 1,000 min		2 different slopes in drawdown curve
P-10	5,100	32.41	3 steady state positions Fluctuation of discharge
EX-3	1,080	8.44	2 different slopes in drawdown and recovery curves
E	8,760	7.89	Recharge effect 2 different slopes in recovery curve
P-6	7,860	38.05	3 steady state positions Fluctuation of discharge
P-14			No clear steady state conditions Fluctuation of discharge Trend to steady state conditions
P-15	9,660	15.47	Recharge effect
P-17	Boundary effect at 500 min		
O.S.	3,180	17.3	Recharge effect
R-4	2,580	5.25	Recharge effect
P-16	4,050	2.46	Recharge conditions 2 different slopes in drawdown curve
M-19	3,960	4.37	Recharge effect
EX-S	3,930	50.97	Recharge effect 2 different slopes in drawdown and recovery curves
H-8	5,730	15.09	Recharge effect 2 different slopes in drawdown and recovery curves
ASR-12	4,290	33.11	Recharge effect
SA-1	3,030	46.23	Recharge effect

Well ID	Time of starting of steady state (min)	Drawdown at steady state (m)	Remarks
AS-11	4,200	3.95	Recharge effect Fluctuation of discharge (1000-4000 min)
Y	2,900	3.15	Recharge effect Fluctuation of discharge (500-2000 min)
M10-R	6,380	8.28	Recharge effect
N-3	2,000	8.82	Recharge effect
B70-1	5,320	16.58	Recharge effect
NWSA	2,850	34.22	Recharge effect
SP	Boundary effect at 300 min		2 different slopes in drawdown curve
M-3	3,900	32.53	Recharge effect
ASR			No recharge effect
HA	Boundary effect at 2,000 min		2 different slopes in drawdown curve
G	3,270	8.67	Fluctuation of discharge at 900 min Steady state in the end of pumping test
D	2,200	1.23	Recharge effect
M19-A	120 min of pumping No recovery data		
D.H.	3,810	64.7	Almost-stability of water levels in end of pumping
KA	3,960		Almost-stability of water levels in end of pumping
P8-R	3,870	31.81	Almost-stability of water levels in end of pumping
TP-1	2,550	33.81	Almost-stability of water levels in end of pumping
AS4-	4,060	8.64	Almost-stability of water levels in end of pumping
AS-1	4,290	86.1	Almost-stability of water levels in end of pumping Volcanics formation 2 different slopes in drawdown curve
H3-R			Fluctuation of discharge No clear steady state Volcanics formation
HZ	Boundary effect at 400 min		2 different slopes in time-drawdown graph Volcanics formation

It is noted that, for the majority of the re-analyzed pumping test results, the drawdown stabilizes when recharge within the zone of influence of the pumped well equals the rate of discharge of the well. No further lowering of water levels will occur as pumping continues at a constant rate. The time-drawdown then becomes horizontal, as in graphs of the majority of listed wells. The first part of curves

in the majority of graphs show that the cone of depression was enlarging during the first time indicated in column 2 of the table. After this time, the cone of depression, or area of influence of the well, encountered a source of recharge. In the second part of the curves, the rate of recharge within the area of influence was sufficient to equal the rate of pumping, resulting in stabilized water levels throughout the area of influence.

There is slow leakage from upper layers of the Tawilah sandstone aquifer. This leakage occurs when an aquifer is in confined conditions. Under ordinary conditions, vertical leakage into the confined aquifer is minimal. During pumping, however, reduction in head within the cone of depression may cause leakage from both above and below the aquifer. Also, there is an impervious boundary in some curves, like a negative boundary. The effect of an impervious boundary on the time-drawdown graph is opposite to the effect of aquifer recharge. The boundary causes the slope of the drawdown plot to steepen instead of flattening.

The comparison between the results of re-analysis and past results are tabulated in Table 5-14.

**Table 5-14 Comparison between the re-analyzed pumping tests results and the past results**

No. Well	Location	X (UTM)	Y (UTM)	Past results		Re-analyzed results	
				T/Drawdown (m <sup>2</sup> /d)	T/Recovery (m <sup>2</sup> /d)	T/Drawdown (m <sup>2</sup> /d)	T/Recovery (m <sup>2</sup> /d)
O.S.	S. Sana'a	416750	1694655	234.185	424.855	113	494
R-4	Rawd Field	415355	1706200	750.16	746.1	435	791
P-16	W. Field	413945	1701124	564.92	1091.9	814 and 174	1110
M-19	Mus.Field	417875	1698860	169.33	95.21	210	210
M-4	Mus.Field	416665	1698207	253.45	63.23	553	443
NWSA	Hasabah	414480	1701500	120.12	105.55	55,3	85,2
EX-S	Haddah	414157	1691674	80.2	89.24	204 and 81.6	340 and 48.6
H-8	Haddah	411300	169090	99.263	129.99	262 and 65.5	655 and 50.4
ASR-12	Assr.Field	410938	1696367	98.78	112.78	85.4	119
SA-1	Zubairy Park	413594	1696222	91.81	414	125	415
AS-11	Assr.Field	410854	1695750	426.53	362.88	873	390
AS4-R	Assr.Field	411868	1695561	204.3	354.6	237	474
Y	E. Field	417084	1700542	911.858	535.84	886	395
N-3	Mus.Field	416455	1700970	180.4	184.3	244	304
M10-R	Mus.Field	44 13 41	15 20 34	300	240	311	514
TP-1	Hasabah	415350	1701200	159	143	264	661
P8-R	W. Field	413000	1705000	48.7	52.023	25.7 and 92.4	34
KA	Kadsia	417245	1693470	177.1	316.4	163	306
DH	W. Field	413470	1706400	28	24.43	20.6	17.1
M19-A	Asbahi	417176	1689477	535.37		510	
D	E. Field	417264	1702475	1476.7	1165.6	615	1840
B70-1	Sabaeen	4141500	1694650	59 and 197.7	179.7	196	613

No. Well	Location	X (UTM)	Y (UTM)	Past results		Re-analyzed results	
				T/Drawdown (m <sup>2</sup> /d)	T/Recovery (m <sup>2</sup> /d)	T/Drawdown (m <sup>2</sup> /d)	T/Recovery (m <sup>2</sup> /d)
G (2002)	E. Field	419194	1702725	1471	260	174	221
HA	Haddah	411005	1691410	314.373	532.16	274 and 137	514
AS-R	Assr.Field	410938	1696367	145.2	190.8	194	173
M-3	Mus.Field	417753	1694599	58.936	44	87	145
SP	Sabaeen Park	414245	1694334	81.1	102.87	123 and 51.6	163
P-17	W. Field	400656	1708837	48	93,06	98.4 and 18.4	88.6
P-14	NW Dahban	410593,86	1706303,7	79	91	90.4	90.4
P-15	Wadi Dahr	409405,26	1709557,5	105	96	105	70.3
P-6	Wadi AL Jabara	413177,6	1702960,7	34	91	32.4	25.6
EX-3	Ssarf	421251	1706952	20.74	19,8	23.7	20.4 and 119
P-10	TV station	413503,83	1703816,1	29	54	33.9	31.6
G-82	Wadi Sawan	419194	1702725	140	373	287 and 115	359
AS-1	Assr.Field	411220	1696100	4,75	3,32	6.33	9.3
HZ	Hizyz	4191766	1685107	24.4	33	28.8 and 14.4	31.6
T	E. Field	417885	1701005	244.5	273	232	310
SS	E. Field	416413,44	1701152,4	3378	3378	3230	2880
M-18	Mus.Field	420320	1698030	216.6	138,693	206	171
W	E. Field	416205	1700850	132.5	137,1	623	121
P-26	W. Field	414109	1700607	92.2	86,6	67.7	65.7
M-16	Mus.Field	441412	152243	280	203	285	474
E	Wadi Sawan	418005	1703262	499	616 and 1825	499	1820
H3-R	Haddah	441158	151841	65	89	14.2	89
P-13	W. Field	413296	1703296	111.15	166	269 and 39.8	299 and 49.8

It is noted from Table 5-14 that there is a difference between the transmissivity value calculated from recovery data and that from pumping data. The estimated transmissivity value from recovery data is higher than the transmissivity calculated from drawdown data. Recall that the time-recovery plot for the pumped well is more accurate than its time-drawdown plot because the residual drawdown measurements are more accurate. During the recovery period, water-level measurements can be made without being affected by pump vibrations and momentary variations in the pumping rate. In analyzing the time-recovery plot, the slope is of primary interest. Two factors determine the slope of the straight line, one is the average pumping rate during the preceding pumping period and the other is the aquifer transmissivity.

Also, increasing the discharge rate during the pumping test causes an increase in the amount of turbulent flow and, thus, a disproportionate increase in the drawdown. As a result, the specific capacity decreases at increasing drawdown. The situation does not reflect the real condition of the well and affect its behavior. Table 5-15 shows the probable causes of the difference between calculated values from both pumping and recovery tests.



**Table 5-15 P probable causes of difference between calculated transmissivity from pumping and recovery tests for some selected re-analyzed pumping test data in Tawilah sandstone aquifer wells in Sana'a Basin**

Well ID	Probable causes
O.S.	Variation of discharge (0 to 30 min) Recharge conditions Head losses: drawdown = 14.27 m at 1 min
R-4	Variation of discharge at 1560 min Recharge conditions
H-8	Effect of boundary and recharge conditions Head losses: drawdown = 7.39 m at 1 min
SA-1	Effect boundary Head losses: drawdown = 13 m at 1 min
AS4-R	Variation of discharge Boundary effect Head losses
Y	Variation of discharge Recharge conditions Head losses
TP-1	Variation of discharge Recharge conditions Head losses: drawdown = 14 m at 1 min
KA	No recharge detected Head losses: drawdown = 14.5 m at 1 min
D	Recharge conditions
B70-1	Variation of discharge Boundary effect and recharge conditions Head losses: drawdown = 11 m at 1 min
HA	Boundary effect Head losses: drawdown = 4 m at 1 min
M-3	Variation of discharge Boundary effect and recharge conditions Head losses: drawdown = 12 m at 2 min
W	Recharge conditions
E	Boundary conditions
H3-R	Variation of discharge Head losses: drawdown = 7.5 m at 1 min

For all wells that show a difference between drawdown and recovery transmissivity values, it is supposed that they are influenced by the following factors:

- Boundary conditions,
- Variation of discharge during pumping test,
- Head losses related to well design.

The head losses are related to design of the wells. An inadequate design creates a large drawdown in the well and thus influences calculation of transmissivity during the pumping test.

#### 5.4.4 Spatial distribution of Tawilah sandstone aquifer constants

The results of new pumping tests carried out in Tawilah sandstone wells (Table 5-11) and the results of the 45 re-analyzed pumping tests (Table 5-14) were used to construct the aquifer constants maps. A brief description of the spatial distribution of each hydraulic constant map is given.

##### a) Hydraulic conductivity distribution map

In general, the Tawilah sandstone aquifer has low regional permeability, while the locally higher permeabilities are found in weathered and fractured zones. The secondary porosity is important in the Tawilah sandstone aquifer and it gives a high permeability to the aquifer. In fractured rocks, the hydraulic conductivity depends on the density and aperture of the joints. The overall hydraulic conductivity of a rock mass is determined by the permeability of the rock matrix and of the fractures. In most cases, the hydraulic conductivity of the fractures is considerably greater than that of the rock matrix so that it is justifiable to neglect the matrix conductivity. The degree of interconnection between fracture clusters is a critical feature that contributes to the hydraulic conductivity of the whole rock mass. It is possible to say that the fracture hydraulic conductivity is a function of fracture size, density, location, aperture, and orientation. The hydraulic conductivity reductions in rocks (especially igneous and metamorphic) vary with depth, having a maximum value at the top and a minimum value at the bottom of the aquifer. The average hydraulic conductivity of the Tawilah sandstone aquifer is determined as 7.3 m/d. Using these values, a hydraulic conductivity contour map is constructed (Figure 5-38). The map shows that the hydraulic conductivity values of the Tawilah sandstone aquifer vary from one place to another. It ranges from 0.5 m/d along the western boundary of the aquifer (well P-20 in the NW direction) to 7 m/d in the south of Sana'a City (latitude 170000 UTM). Generally, it decreases in the E-W direction. Two anomaly values of K are well developed, one in the middle of the aquifer (NW NWSA well fields) while the second is in the center of Sana'a Plain. The occurrence of these anomaly values is governed by the lithologic composition of the aquifer sediments, as well as the structure and its thickness. The lowest values are located in the south of the aquifer.

##### b) Transmissivity distribution map

Transmissivity calculated from recovery data reflects the behavior of the aquifer. The transmissivity of the wells penetrating the Tawilah sandstone aquifer exhibits a great variation. It ranges from 6 to 3,770 m<sup>2</sup>/d. This great variation may be attributed to the effects of fissuring caused by faulting and/or by intrusion of igneous dykes. About 18% of the calculated transmissivity values are more than 500 m<sup>2</sup>/d, while about 80% range between 50 and 500 m<sup>2</sup>/d (Table 5-16). This means that the aquifer potentiality ranges between moderate to high (Table 5-17). The potential of the aquifer may be attributed to the degree of fracturing in the Tawilah sandstone aquifer.

**Table 5-16 Ranges of calculated transmissivity values in re-analysed pumping tests of Tawilah sandstone aquifer wells in Sana'a Basin (Total number of wells = 81)**

Range	Number of wells	Percentage
From 0 to 100 m <sup>2</sup> /d	30	37%
From 101 to 200 m <sup>2</sup> /d	15	19%
From 201 to 300 m <sup>2</sup> /d	5	6%

Range	Number of wells	Percentage
From 301 to 400 m <sup>2</sup> /d	9	11%
From 401 to 500 m <sup>2</sup> /d	7	9%
From 501 to 600 m <sup>2</sup> /d	7	9%
From 601 to 700 m <sup>2</sup> /d	3	3%
From 701 to 4000 m <sup>2</sup> /d	5	6%

**Table 5-17 Ranges of aquifer potential (Zekai Sen, 1995)**

Transmissivity (m <sup>2</sup> /d)	Potentiality
T>500	High
500<T<50	Moderate
50<T<5	Low
5<T<0,5	Weak
T<0,5	Negligible

Spatial distribution of transmissivity in the eastern part of the Tawilah sandstone aquifer (Figure 5-39) shows a general trend of increase from east to west, while a reverse direction arises west of Sana'a City. This may be attributed to the degree of cementation and compaction, as well as to the structural effect. The degree of cementation and compaction can be changed at the same formation locally as a result of hydrothermal processes noted in the Lower Cretaceous sandstone. In general, in the western part of the aquifer, the wells with high transmissivity values are oriented in a SE-NW direction following a large structure that affects the aquifer, probably a fault.

In conclusion, structural geology governs the transmissivity of the Tawilah sandstone aquifer and causes heterogeneity of the aquifer. The degree of fracturing is the main element and it determines the potentiality of this aquifer. The orientation of main structures in the Sana'a Basin is related the high potentiality of the Tawilah sandstone aquifer. Furthermore, in the fractured sandstone aquifer, it is difficult to assess the saturated thickness of aquifer, as well as the hydraulic conductivity of the aquifer.

**c) Storage coefficient distribution map**

The spatial distribution of the storage coefficient map of the Tawilah sandstone aquifer was constructed based on the available new and re-analyzed data (Table 5-18). The table shows that the storage coefficient of this aquifer ranges between  $1.47 \times 10^{-4}$  (well ID GW-2) and  $9.35 \times 10^{-3}$  (well ID SE-7). The storage coefficient map of the Tawilah sandstone aquifer (Figure 5-40) shows that the relatively high values of storage coefficient are estimated in the western part of the aquifer, while the relatively low values are characteristic of the southern parts of the aquifer. This may be attributed to the impact of the structure density characterizing the western part of the aquifer more than that in the southern part. The spatial distribution of the storage coefficient in this aquifer shows a general trend of increase from NW to SE direction, while the opposite is the case from SE to NW direction. In general, due to the limited data upon which the map was constructed, there aren't sufficient contour lines to show the trend of increase of storage coefficient in the other parts of the aquifer.

**Table 5-18 Results of estimated storage coefficient in the Tawilah sandstone aquifer in Sana'a Basin**

Well number	Aquifer formation	Storage coefficient
P-17	Tawilah Formation	$2.07 \times 10^{-3}$
P-15	Tawilah Formation	$0.93 \times 10^{-3}$
P-8	Tawilah Formation	$2.08 \times 10^{-4}$
P-16	Tawilah Formation	$6.1 \times 10^{-4}$
sF (OW)	Tawilah Formation	$3.9 \times 10^{-3}$
P-17 (OW)	Tawilah Formation	$1.855 \times 10^{-3}$
SE-1 (OW)	Tawilah Formation	$1.8 \times 10^{-4}$
SE-2 (OW)	Tawilah Formation	$3.84 \times 10^{-4}$
SE-3 (OW)	Tawilah Formation	$7.52 \times 10^{-4}$
Iraqi Well (OW)	Tawilah Formation	$4.43 \times 10^{-4}$
SE-7 (OW)	Tawilah Formation	$9.35 \times 10^{-3}$
SE-5 (OW)	Alluvial formation	$3.82 \times 10^{-4}$
ST-7 (OW)	Tawilah Formation	$7.65 \times 10^{-3}$
GW-2 (OW)	Tawilah Formation	$1.47 \times 10^{-4}$
WM 425S (OW)	Tawilah Formation	$4.447 \times 10^{-3}$



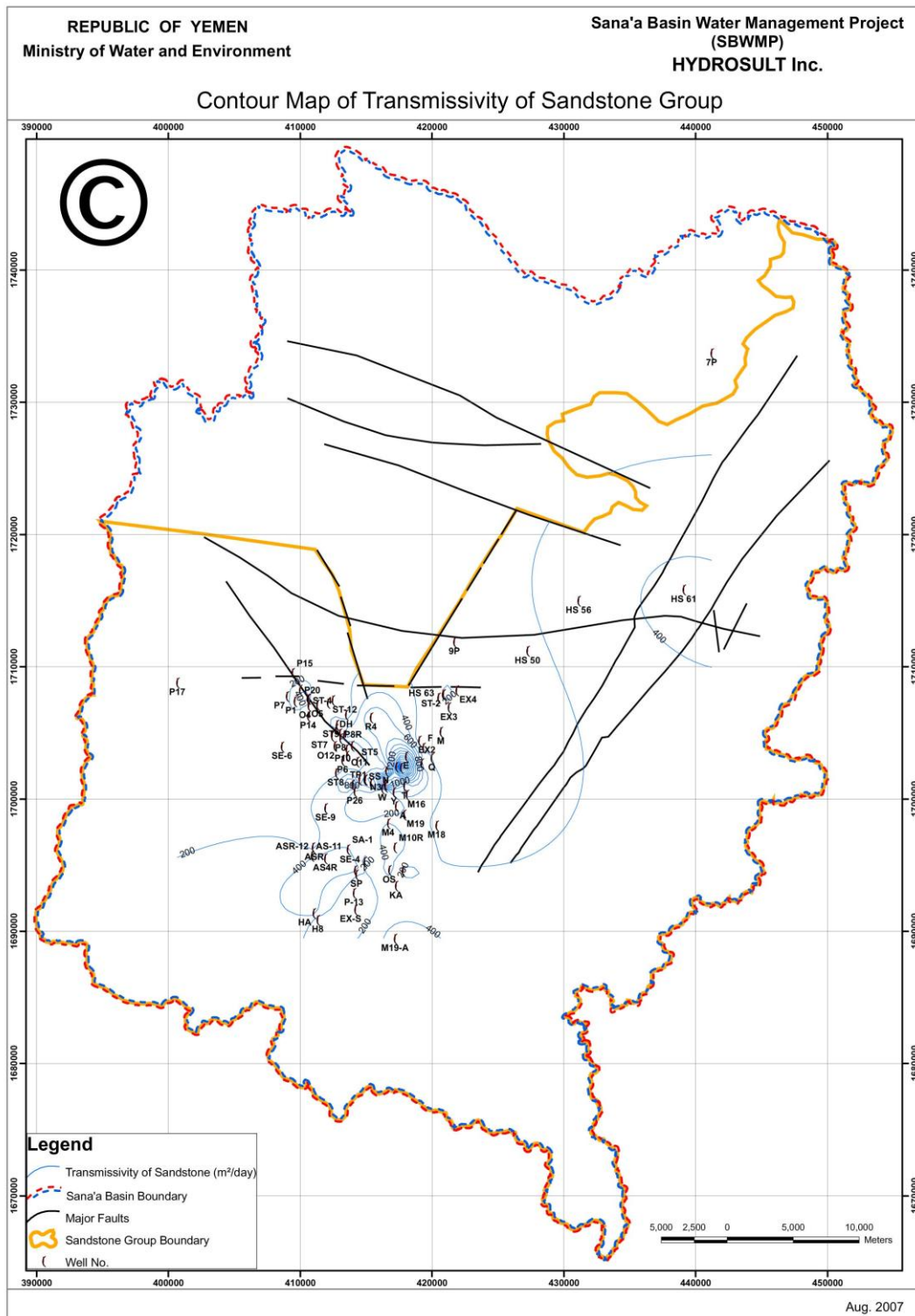


**Figure 5-40 Transmissivity distribution zonation map of the Tawilah sandstone aquifer in Sana'a Basin**

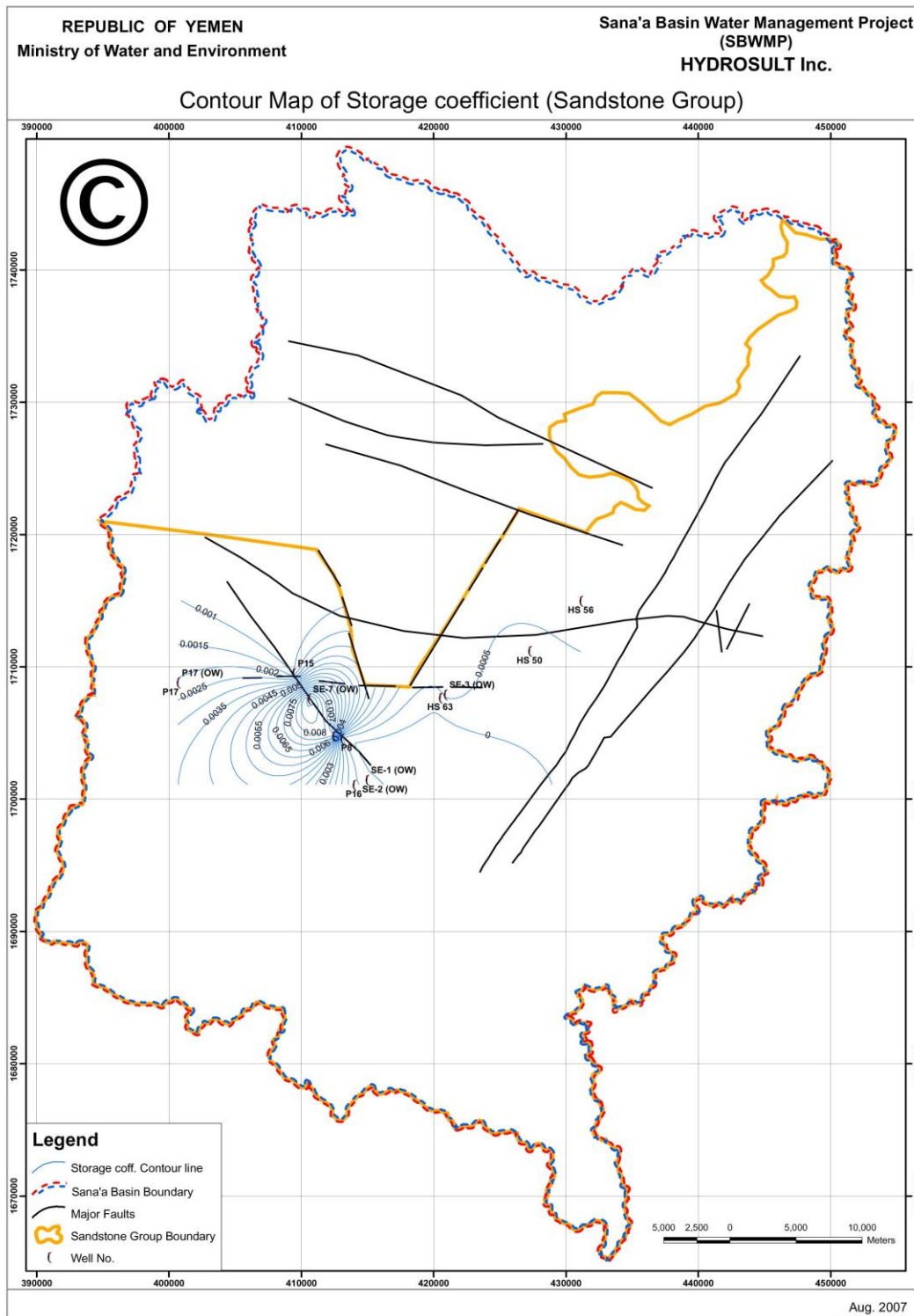


**Figure 5-41 Storage coefficient distribution zonation map of the Tawilah sandstone aquifer in Sana'a Basin**

## 5.5 Conclusions

The assessment of hydrodynamic characteristics of alluvium, Tawilah sandstone and volcanic aquifers from new pumping tests and data from past pumping tests on record reflects the following:

- The Tawilah sandstone aquifer is the main aquifer in the Sana'a Basin;
- Past pumping test data are concentrated around the Sana'a Plain and concern the Tawilah sandstone aquifer. Statistical study of hydrodynamic characteristics shows that the Tawilah sandstone aquifer is highly anisotropic and heterogeneous in relation to structural events that affect this aquifer. The range of transmissivity is very wide for the same formation. This may be attributed to the degree of fracturing that affects the aquifer;
- There is no correlation between different hydrodynamic parameters of the Tawilah sandstone aquifer, such as depth versus transmissivity or thickness of aquifer versus transmissivity;
- Transmissivity of the volcanics aquifer also depends on the degree of fracturing;
- Analysis of pumping test curves from the Tawilah sandstone aquifer shows that there is a lateral recharge effect. This recharge comes from the same aquifer, but from a long distance;
- In the Ghatrane area, the geological structure constitutes a boundary effect and limits the hydraulic relationship between wells in the Tawilah sandstone aquifer. In the Bani Hushaish area, the effect of geologic structures, such as dykes, is pronounced in the pumping tests;
- The storage coefficient indicates that the Tawilah sandstone aquifer is under confined conditions ( $S$  varies between  $10^{-4}$  and  $10^{-3}$ ) in the area around the Sana'a Plain and in Bani Hushaish;
- Groundwater in the shallow zone of the Tawilah sandstone aquifer is generally stored under unconfined conditions (water-table) although the overlying poorly permeable alluvium or silt-clay layers inter-bedded with the Tawilah sandstone may impart some degree of confinement to the aquifer. Where the sandstone is overlain by a considerable thickness of alluvium, confined to semi-confined conditions prevail with storage coefficients of the order of  $10^{-4}$ .